World Journal of Hepatology

Submit a Manuscript: http://www.wjgnet.com/esps/
Help Desk: http://www.wjgnet.com/esps/helpdesk.aspx
DOI: 10.4254/wjh.v7.i16.1987

World J Hepatol 2015 August 8; 7(16): 1987-2008
ISSN 1948-5182 (online)

REVIEW

Focal liver lesions: Practical magnetic resonance imaging approach

António P Matos, Fernanda Velloni, Miguel Ramalho, Mamdoh AlObaidy, Aruna Rajapaksha, Richard C Semelka

António P Matos, Fernanda Velloni, Miguel Ramalho, Mamdoh AlObaidy, Aruna Rajapaksha, Richard C Semelka, Department of Radiology, University of North Carolina, Chapel Hill, NC 27599-7510, United States

António P Matos, Miguel Ramalho, Department of Radiology, Hospital Garcia de Orta, 2801-951 Almada, Portugal

Mamdoh AlObaidy, Department of Radiology, King Faisal Specialist Hospital and Research Center, Riyadh 11461, Saudi Arabia

Author contributions: All authors have contributed equally to this work in form of literature review, manuscript writing/editing, and figure collection/illustration/annotation/captioning.

Conflict-of-interest statement: There is no conflict of interest associated with any of the senior author or other coauthors contributed their efforts in this manuscript.

Correspondence to: Richard C Semelka, MD, Professor, Department of Radiology, University of North Carolina, UNC at Chapel Hill CB 7510 - 2001 Old Clinic Bldg., Chapel Hill, NC 27599-7510, United States. richsem@med.unc.edu
Telephone: +1-919-9669676
Fax: +1-919-8437147

Received: April 18, 2015
Peer-review started: April 18, 2015
First decision: June 18, 2015
Revised: June 24, 2015
Accepted: July 23, 2015
Article in press: July 27, 2015
Published online: August 8, 2015

Abstract

With the widespread of cross-sectional imaging, a growth of incidentally detected focal liver lesions (FLL) has been observed. A reliable detection and characterization of FLL is critical for optimal patient management. Maximizing accuracy of imaging in the context of FLL is paramount in avoiding unnecessary biopsies, which may result in post-procedural complications. A tremendous development of new imaging techniques has taken place during these last years. Nowadays, Magnetic resonance imaging (MRI) plays a key role in management of liver lesions, using a radiation-free technique and a safe contrast agent profile. MRI plays a key role in the non-invasive correct characterization of FLL. MRI is capable of providing comprehensive and highly accurate diagnostic information, with the additional advantage of lack of harmful ionizing radiation. These properties make MRI the mainstay for the noninvasive evaluation of focal liver lesions. In this paper we review the state-of-the-art MRI liver protocol, briefly discussing different sequence types, the unique characteristics of imaging non-cooperative patients and discuss the role of hepatocyte-specific contrast agents. A review of the imaging features of the most common benign and malignant FLL is presented, supplemented by a schematic representation of a simplistic practical approach on MRI.

Key words: Malignant; Benign; Magnetic resonance imaging; Focal liver lesions; Hepatobiliary contrast agents

Core tip: With the widespread of cross-sectional imaging, a growth of incidentally detected focal liver lesions (FLL) has been observed. A reliable detection and characterization of FLL is critical for optimal patient management. Magnetic resonance imaging

(MRI) plays a key role in non-invasive characterization of FLL. The multiparametric ability of pre- and post-contrast sequences is an intrinsic advantage of MRI to reach an accurate diagnosis. New techniques such as diffusion-weighted sequences and hepatocyte-specific contrast agents are being currently used in clinical practice, which might further improve the detection and characterization of FLL.

Matos AP, Velloni F, Ramalho M, AlObaidy M, Rajapaksha A, Semelka RC. Focal liver lesions: Practical magnetic resonance imaging approach. *World J Hepatol* 2015; 7(16): 1987-2008 Available from: URL: http://www.wjgnet.com/1948-5182/full/v7/i16/1987.htm DOI: http://dx.doi.org/10.4254/wjh.v7.i16.1987

INTRODUCTION

With the widespread of cross-sectional imaging, a growth in rate of incidentally detected focal liver lesions (FLL) has been observed. A reliable detection and characterization of FLL is critical for optimal patient management. The majority of FLL arising in noncirrhotic liver are benign[1], even in patients with known extra-hepatic malignancy. Cysts, hemangiomas, focal nodular hyperplasias (FNH), and hepatocellular adenomas (HCA) are the most commonly encountered benign lesions[1-5]. The most commonly encountered malignant lesions in noncirrhotic liver are metastases[6-8]. Hepatocellular carcinomas (HCC), and to a lesser extent intrahepatic cholangiocarcinomas (IHC), occur mainly in the setting of chronic liver disease, and represent the most common primary liver malignancies[7,9-14].

A tremendous development of new imaging techniques has taken place during these last years. Maximizing accuracy of imaging in the context of FLL is paramount in avoiding unnecessary biopsies, which may result in post-procedural complications up to 6.4%, and mortality up to 0.1%[15-17]. Nowadays, magnetic resonance plays a key role in management of liver lesions, using a radiation-free technique and a safe contrast agent profile[18,19].

The heightened soft-tissue resolution and sensitivity to intravenous contrast agents provided by magnetic resonance imaging (MRI) makes it an invaluable problem-solving tool for fully characterizing FLL[20,21]. Previous studies estimated the sensitivity and specificity of MRI for the diagnosis of FLL of 94% and 82%-89%, respectively[22].

This review focuses on the diagnostic performance of MRI in evaluating the most common benign and malignant FLL. As a summary, a practical educational approach to FLL on MRI is also presented.

MRI PROTOCOL

With the current state of the art technology, magnets of 1.5 Tesla (T) and 3T field strength are considered the standard of reference in providing high-quality and consistent MR images. Giant advances in MRI have been achieved in the last decade in regards to each of the following: hardware (high-performance gradient coils and phased-array surface coils), software (new sequence design and new parallel imaging technology and acceleration techniques), and contrast agents (hepatocyte-specific agents) have made a major impact on imaging of the liver.

In our perspective, an adequate imaging protocol has to be short, comprehensive, and standardized to allow reproducibility and consistency of image quality and diagnostic performance. A comprehensive protocol allows the evaluation of the parenchyma, vasculature, and biliary system; by using either breathing-independent sequences or breath-hold sequences that minimize motion artifact and spatial misregistration. Gradient-echo (GRE) sequences generally are used in T1-weighted sequences and fast spinecho sequences are used in T2-weighted sequences[20,23].

The state of the art MRI protocols rely on a combination of fat-suppressed and non-fat-suppressed T2-weighted images (T2-WI), in- and opposed-phase (IP/OP) T1-WI and dynamic pre- and post-contrast fat-suppressed T1-WI[7,12].

The predominant information provided by T2-WI is about fluid content, fibrotic tissue and iron content (reflected by high, low, and very low signal intensity, respectively). Fat suppression is generally applied for at least one set of images in order to increase lesions conspicuity.

Pre-contrast T1-WIs are extremely important in lesion characterization. Most FLL are mildly or moderately low in signal intensity. Lesions with high-fluid or fibrous tissue content are moderately or substantially low in signal intensity. Hemorrhagic lesions, and those with high protein or fat content, are high in signal intensity on T1-WI. Fat suppression technique facilitates reliable characterization of fatty lesions. GRE sequences provide T1-WI in a short amount of time and allow chemical shift imaging in a single breath-hold (dual echo acquisition). The two echo times are chosen so that fat and water peaks are IP and OP, respectively. OP images are useful to detect small amounts of intracellular fat in liver lesions and in hepatic parenchyma. If fat and water are in the same voxel, the signal intensity decreases on the OP images, with maximal signal loss occurring when fat and water are in equal proportion.

Gadolinium-enhanced images are performed routinely in a multiphasic dynamic fashion, using three-dimensional (3D) fat-suppressed GRE breath-hold T1-WI. The acquired phases include late arterial, portal venous, interstitial, and delayed phases; which allow the assessment of enhancement kinetics (a reflection of both vascularity and permeability). However, most diagnostic information can be derived from the late hepatic arterial phase, also called hepatic-arterial dominant phase, with the correct timing characterized by observing contrast enhancement in the portal vein branches and no enhancement in the hepatic veins[24]. Suggested

Table 1 Comparison between extracellular and hepatocyte-specific agents (Multihance® and Eovist®)

	Extracellular contrast agents	Hepatocyte-specific agents	
		Multihance®	Eovist®
Advantages	Robust arterial and portal venous phase imaging	Robust arterial and portal venous phase imaging	Hepatobiliary imaging
	Price and availability	Hepatobiliary imaging	Short delay for hepatobiliary phase (20 min)
		Smaller dose administration	Smaller dose administration
		Safer for renal impaired patients	Safer for renal impaired patients
		Price	
Disadvantages	No hepatobiliary phase	Availability (not available in all countries)	Less robust arterial and portal venous phase imaging
	NSF cases reported with less stable agents	Longer delay for hepatobiliary phase (90-180 min)	Pitfalls for inexperienced readers
			Price

methods for ensuring an optimal arterial phase liver MRI have varied between empiric fixed delay or individually-tailored timing. The latter method is recognizable to be more accurate and with improved reproducibility, and involves either pre-scanning with a test bolus, or tracking bolus arrival in the descending aorta[25]. In our practice, a bolus-tracking technique (CARE bolus software) is employed to capture the late hepatic arterial phase. This is performed by the technologist, who, when visualizing maximum aortic enhancement at the level of celiac trunk, will provide an 8 s breath-holding instructions prior to initiating the scan.

Adequate delay between initiation of contrast injection and initiation of the sequence is crucial to aid in optimizing the detection of hypervascular lesions. The precision in timing the portal venous phase is more flexible and less critical (45-75 s), characterized by enhancement of the entire hepatic vascular system. The portal venous phase maximizes contrast between hypovascular lesions and the background liver, and can be used to evaluate the contrast washout pattern, which is a useful discriminating feature. Images acquired 1.5 to 10 min after contrast injection are in the interstitial/delayed phase of enhancement, which aid in evaluating persistent enhancement in hemangiomas, washout in HCC, or delayed enhancement of fibrotic tissue or tumors, such as in cases like cholangiocarcinoma.

Intravenous MR contrast agents can be divided into extracellular (ECA) and hepatocyte-specific agents (HSA). ECA equilibrate with the extracellular fluid space after intravenous injection and are excreted by glomerular filtration, similar to computed tomography (CT) agents. This permits multi-phase dynamic post-contrast imaging as described earlier.

Like ECA, HSA allow the multi-phase dynamic post-contrast imaging. Moreover, they show some degree of biliary excretion, allowing a late hepatobiliary phase acquisition. Due to the action of known cellular membrane transporters, only normal functioning hepatocytes take up HSA and excrete them to the biliary tree[26]. Hepatobiliary phase images are easy to recognize because both the liver and the bile ducts are markedly enhanced. The blood vessels as well as all non-hepatocellular lesions and lesions with impaired hepatocytes all appear hypointense.

The two HSA available are Eovist® (gadoxetic acid, Bayer Health-Care Pharmaceuticals, marketed as Primovist® outside the United States) and MultiHance® (gadobenate dimeglumine, Bracco). With Eovist®, 50% of the dose is taken up by hepatocytes and eliminated by biliary excretion, compared to 3%-5% with MultiHance®. Hepatobiliary phase images are acquired 20-40 min after Eovist® injection, compared to 1.5-3 h after MultiHance® injection. Advantages and disadvantages of these agents and extracellular contrast agents are shown in Table 1.

The substantial difference on the biliary elimination of Eovist® compared to the other contrast agents affects the classical MR technique, lesion appearance, and thus image interpretation[27]. These differences provide not only advantages on detection and lesion characterization, but also new pitfalls in imaging interpretation[27]. The advantages in the evaluation of FLLs are appreciated in the distinction between FNH and HCA, and in the diagnosis of HCC and metastasis; while the pitfalls are related to the less favorable behavior as an extracellular agent and the "pseudowashout" of benign lesions[27]. Washout is historically linked to malignant lesions, particularly to hypervascular metastases and HCC. While using Eovist®, the "pseudowashout" may pose a risk in the diagnosis of benign lesions. As an example, hemangiomas are classically described as hypervascular lesions with centripetal fill-in, sustained in late dynamic postcontrast phases. With Eovist®, the accumulation of contrast can be masked by the intense hepatic parenchymal enhancement, giving the "illusion" of washout of the hemangioma[27].

At our center, we use MultiHance® as the standard contrast agent since it shows better enhancement on dynamic evaluation[26,28], and reserve Eovist® for selected cases on a problem-solving basis.

Recently, diffusion-weighted imaging (DWI) sequences have been shown to be an emerging contributor for liver MRI[29-32] and are being incorporated in most abdominal MR protocols. Diffusion is a physical process of random movement of water molecules. This movement of intracellular water molecules is restricted by the presence of cell membranes. In highly cellular tissues, such as neoplasms, diffusion is restricted due to the

relative larger intracellular volume and high density of cellular membranes. DWI exploits this phenomenon and its image contrast is based on differences in the mobility of water protons (as a measure of cellularity), between different tissues[31]. This MR technique should be used in combination with conventional unenhanced and contrast-enhanced MRI. It is especially useful in patients with contraindication to gadolinium contrast agents[32].

Additional sequences may be added to the protocol on specific clinical settings. For diffuse deposition diseases, fat-quantification or T2 star (T2*) sequences can be added.

Despite all development in MRI, its diagnostic performance is still affected by motion artifacts, which may result in inconsistent image quality. Motion artifacts, especially those produced by physiological motion caused by patient respiration, may distinctly degrade the quality of MR images. In patients who are unable to cooperate with breath-hold instructions, the sequences that are more affected are the T1-weighted GRE sequences. In order to minimize these artifacts, new motion-robust sequences have been implemented. The magnetization-prepared rapid gradient-echo (MP-RAGE) sequence is a 2D, single-section acquisition technique that can be used to obtain motion-free and moderate quality images. The acquisition times per-section are as short as 1 s[33]. These sequences can be used pre- and post-contrast. Additionally, a recently described new application of MP-RAGE IP/OP images is able to replace standard dual-echo chemical shift imaging with moderate to good image quality[34]. Recent developments in MR data sampling and *k*-space filling have been used to acquire 3D-GRE T1-WI. Radial data sampling 3D GRE can be used as a free-breathing sequence, providing high-quality pre- and post-contrast images[2,34,35]. The major drawback of radial 3D-GRE is the long acquisition time and therefore low temporal resolution of this technique. Until now, conventional radial 3D-GRE sequence is unable to provide, in a consistently fashion, critical scanning phases, *i.e.,* the late hepatic arterial phase. New sequences are being developed in order to provide a compromise between spatial and temporal high-resolution images, with reduced acquisition time and increased motion resistance.

BENIGN LESION

Hemangiomas

Hemangiomas are tumors of mesenchymal origin and are the most common benign liver solid lesions. The prevalence of these lesions ranges from 1%-20%, more frequently between fourth and fifth decade of life, showing a female predilection (ratio of 2-5:1)[36-38]. The size of hemangiomas usually remains stable and can vary from a few millimeters to more than 20 cm[38]. Complications are rare, and large lesions may become symptomatic due to compression of adjacent structures, rupture, or spontaneous hemorrhage[13].

On MRI, the majority of hepatic hemangiomas display pathognomonic pre- and post-contrast imaging features (Figure 1) enabling a correct diagnosis with high accuracy[39,40]. Frequently, hemangiomas show moderately high signal intensity on T2-WI, usually less bright than simple cysts or cerebrospinal fluid, and low signal intensity on T1-WI[1,41]. On post-contrast images, a nodular or "flame-shaped", discontinuous, peripheral enhancement is observed, as well as late, progressive, centripetal filling, and persistent delayed enhancement, similar to that of hepatic vessels. Larger hemangiomas may show incomplete filing along the dynamic imaging due to central scarring. Conversely, small (< 2 cm) hemangiomas may show rapid complete filling on the late arterial phase images. Subcentimeter hemangiomas may fade to isointensity to the background liver parenchyma in interstitial phase images; however, they never washout. On the arterial phase, especially the small rapidly enhancing subcapsular hemangiomas may show a perilesional enhancement[40], and this finding should not be regarded as an atypical or suspicious feature. Nevertheless, hemangiomas may uncommonly show atypical morphologic characteristics. The possible atypical findings are scarring, septations, capsular retraction, calcifications, cystic transformation and fluid-fluid level. Extremely rare is the interval growth, imposing the exclusion of other diagnostic possibilities, namely malignancy[14,38,41]. The end stage of a hemangioma involution results in appearance of hyalinized or sclerosed hemangiomas. At this point these lesions lose the homogeneous high signal intensity on T2-WI and the typical globular enhancement may not be seen[38,41]. As stated above, it should be emphasized that, when using Eovist®, small rapid filling hemangiomas will not show the typical features described earlier during the late interstitial phase due to the rapid uptake of contrast by the background liver parenchyma, giving the illusion of washout. Furthermore, hemangiomas will not show any uptake on the hepatobiliary phase, and will show the same appearance as non-hepatocytes containing lesions, *e.g.*, cysts, metastasis, and to a lesser extent HCA[28,38].

Focal nodular hyperplasia

FNH consists of a non-encapsulated lesion composed by non-neoplastic hepatocytes in a disorganized array, surrounding a central fibrous scar with a dystrophic arterial vessel[5,7,42]. There is some histopathologic heterogeneity of FNHs, with uncommon "non-classical" histologic subtypes described in the literature[42,43]. FNH is the second most common solid benign FLL. Most often found in young and middle-aged patients, FNH has a clear female predominance (8-12:1 ratio)[1,42].

MRI is considered the best imaging tool for FNH diagnosis, with a sensitivity of 70% and a specificity of 98%[44]. For some authors, contrast-enhanced MRI is considered the gold standard[5]. As FNH are composed of hepatocytes, they are barely discernable from normal parenchyma on precontrast images, appearing iso- or hypointense on T1-WI, and iso- or slightly hyperintense

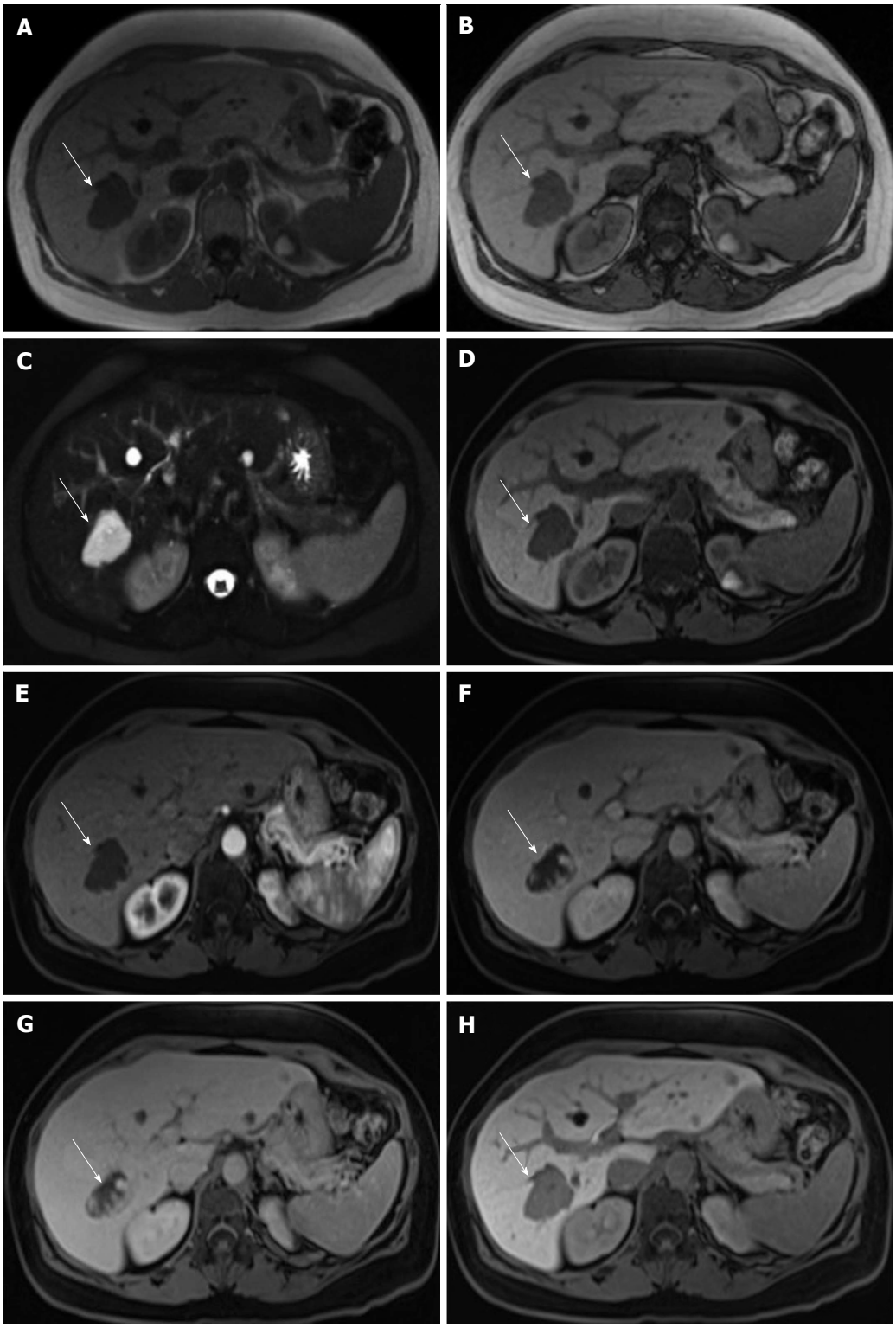

Figure 1 Hemangioma. In (A) and opposed-phase (B) GRE T1-WI, fat-suppressed FSE T2-WI (C), pre (D) and post hepatocyte-specific contrast agent (Eovist®) fat-suppressed 3D-GRE T1-WI at the arterial (E), portal venous (F), interstitial (G) and hepatobiliary (H) phases. There is a lobulated lesion on the right hepatic lobe (arrows), showing marked low signal intensity on T1-WI (A, B and D) and marked high signal intensity on T2-WI (C). The lesion demonstrates peripheral and discontinuous nodular enhancement (E), which become larger and coalescent on delayed postcontrast images (F and G), showing a progressive centripetal filling. Due to the absence of hepatocytes, hemangiomas show low signal intensity on the hepatobiliary phase (H), acquired 20 min after the administration of the hepatocyte-specific contrast agent. GRE: Gradient-echo; FSE: Fast spinecho; T1-WI: T1-weighted images.

on T2-WI. In approximately 50%-84% of cases, the central scar can be seen with low signal intensity on T1-WI and moderate high signal on T2-WI[42,44]. On postcontrast images, FNHs show typical enhancement pattern: early arterial homogeneous enhancement, which becomes isointense to the background liver on portal venous phase, and late enhancement of the central scar (Figure 2). No washout is seen with FNH[43,44].

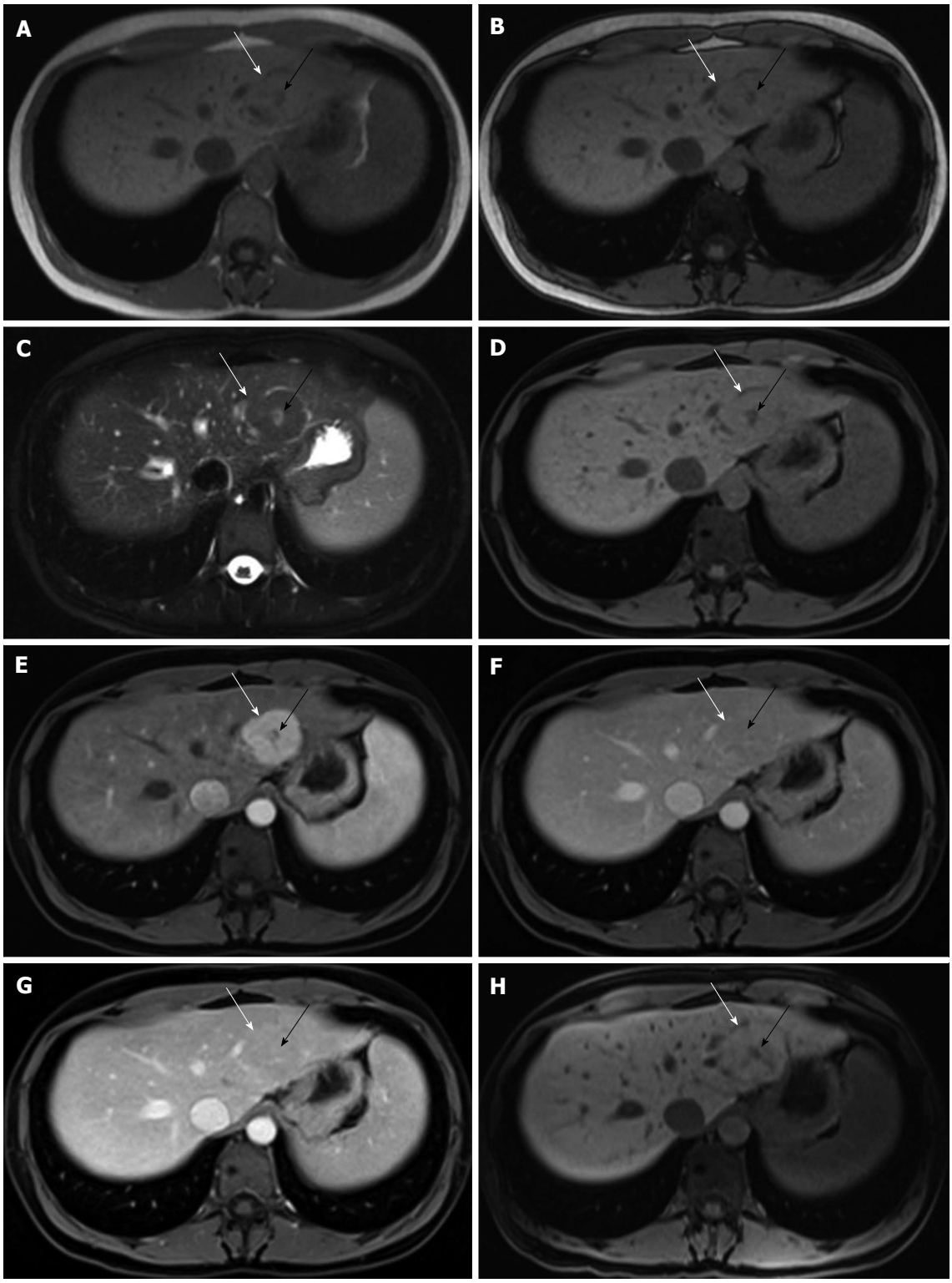

Figure 2 Focal nodular hyperplasia. In- (A) and opposed-phase (B) GRE T1-WI, fat-suppressed FSE T2-WI (C), pre (D) and post hepatocyte-specific contrast agent (Eovist®) fat-suppressed 3D-GRE T1-WI at the arterial (E), portal venous (F), interstitial (G) and hepatobiliary (H) phases. There is a lesion on the left hepatic lobe (white arrow, A-H), showing isointense signal comparing to the surrounding liver on non-contrast T1-WI (A, B and D) and on T2-WI (C). The lesion also shows a central scar (black arrow, A-H), which is hypointense on T1-WI (A, B and D) and hyperintense on T2-WI (C). The lesion demonstrates homogeneous enhancement on early post-contrast images (E), becoming isointense to the underlying liver parenchyma (F and G). The progressive enhancement of the central scar is depicted on the delayed post-contrast images (G). On the hepatobiliary phase, 20 min after the administration the hepatocyte-specific contrast agent, the lesion shows uptake of the contrast agent, becoming minimally hyperintense comparing to the surrounding liver parenchyma. Since the central scar has no hepatocytes, there is no uptake of the contrast agent, becoming hypointense comparing to the liver and to the rest of the lesion. GRE: Gradient-echo; FSE: Fast spinecho; T1-WI: T1-weighted images.

The prevalence of typical features of FNH in literature ranges from 22%-70%[44], mainly related to different study designs and histopathologic heterogeneity of these lesions[43]. Using HSAs, the presence of normal

functioning hepatocytes can be demonstrated. Unlike the majority of HCA, FNHs show, on the vast majority of cases, iso- or hyper-enhancement on the hepatobiliary phase[1,7,45].

HCA

HCA is an uncommon benign primary FLL, and most often encountered in women of childbearing age taking oral contraceptives. Unlike FNH, HCAs are true neoplasms, defined as the monoclonal proliferation of well-differentiated hepatocytes arranged in sheets and cords. They lack portal triads and interlobular bile ducts. Nowadays, according to their genotypic and phenotypic characteristics HCAs are classified into 3 major molecular subtypes[5,46]: (1) inflammatory (formerly known as telangiectatic FNHs); (2) hepatocyte nuclear factor 1-alpha (HNF-1α) inactivated; and (3) Beta (β)-catenin-activated lesions. A fourth group can be considered including those HCAs that are unclassified in the previous subtypes. As different groups have distinct probability for HCC transformation, a pre-operative diagnosis is ideal for an appropriate patient management.

Generally, on MRI HCAs show mild to moderate high signal intensity on T2-WI and enhancement on the late arterial phase on post-contrast sequences (Figure 3). HCA do not show uptake on hepatobiliary phase with HSA. Although further validation is required, specific MRI features can be used to identify HCA subgroups[47-49]. Inflammatory HCAs (50%) tend to show peripheral marked high signal on T2-WI and maintained enhancement on more delayed images[1,47,49]. HNF-1α-inactivated HCAs (35%-45%) show diffuse intralesional fat deposition, responsible for higher signal intensity on non-fat-suppressed T1-WI and drop of signal on OP images. β-catenin-activated HCAs (10%-15%) findings are less defined, showing vaguely defined scars or poorly defined areas of high signal on T2-WI. For the first two subgroups (majority of adenomas), MRI have specificities ranging from 88%-100%[3,49]. These HCAs have null or extremely low probability of HCC transformation. β-catenin-activated HCAs have a high probability of malignancy transformation[5,46,48].

Sometimes MRI features of HCAs can overlap with FNHs. Distinctive features should be stressed. HCAs rarely show a central scar and much more frequently depict intralesional fat[44]. Homogeneity strongly suggests FNH over HCA[44]. The utilization of HSA is recommended to help in the distinction between FNH and HCA. The former showing increased uptake on hepatobiliary phase, while HCAs, usually, show no enhancement[4,28,50].

Benign cystic lesions

Cystic benign liver lesions are common and may represent a broad spectrum of entities ranging from developmental cysts to neoplastic lesions. It is important to distinguish them from malignant lesions that can show cystic transformation (as metastases or hepatocellular carcinoma). Fluid-containing benign liver lesions can be grouped broadly into simple or complex cysts[51].

The differential diagnosis of simple cysts includes benign developmental hepatic cysts, biliary hamartomas, foregut cysts, Caroli disease, and adult polycystic liver disease[51]. The benign developmental hepatic cyst shows homogeneously low signal on T1-WI and homogeneously strong high fluid signal on T2-WI (Figure 4). The margins are well defined and no enhancement is shown on postcontrast sequences. Biliary hamartomas are usually small (< 1.5 cm), round or irregular, and may show very thin and uniform peripheral enhancement (Figure 5), due to compressed liver parenchyma[52,53]. They have no connection to the biliary tree. Conversely, in Caroli disease the varying size cysts communicate with the biliary tree. Communication with the biliary system can be further confirmed using dedicated cholangiographic sequences or HSAs. The cysts depicted on adult polycystic liver disease appear as benign developmental hepatic cysts. MRI is the best modality for identifying cysts complicated by hemorrhage or infection[52].

Benign complex cysts are traumatic, inflammatory, or neoplastic in nature. Traumatic cystic lesion may occur after blunt or penetrating trauma, or iatrogenic injury, such as after cholecystectomy or liver surgery. On MRI, bilomas and seromas may resemble simple cysts, while hematomas show different intensity based on the age of the blood products[52].

The most frequent inflammatory cystic lesions are abscesses and hydatid cysts. With the advent of effective antimicrobial therapy, currently biliary tract pathologies have surpassed portal seeding from appendicitis and diverticulitis, as the most common source of pyogenic liver abscesses[54]. Abscesses are thick-walled lesions with low signal intensity on T1-WI and high signal intensity on T2-WI, with progressive enhancement of the wall[1]. Adjacent parenchyma shows high signal on T2-WI (edema) and enhancement on the arterial phase, due to inflammatory reaction[1,52,55] (Figure 6). Hydatid cysts are due to Echinococcus infestation. On MRI, daughter cysts and internal septa are readily visualized on T2-WI. Most echinococcal cysts show variable low to high signal intensity on T1-WI, depending on the amount of proteinaceous debris, and markedly high signal on T2-WI. The fibrotic component and the presence of calcifications appear as a hypointense pericystic rim, on both T1- and T2-WI. Cyst walls and internal septa enhance on post-contrast images[55].

Although rare, biliary cystadenoma (BCA) is the most frequent benign cystic neoplasm. It has biliary origin, with most of them (85%) arising from the intrahepatic bile ducts[1,55]. BCA usually appear as large (mean 12 cm; range 3-40 cm), well-defined and multi-loculated intrahepatic cyst. On MRI, BCAs typically show high signal on T2-WI and show variable T1 signal intensity due to proteinaceous content or blood products. Septal or mural calcifications (depicted as signal voids on all sequences) and fluid-fluid levels are occasionally seen. Post-contrast sequences may demonstrate enhancement

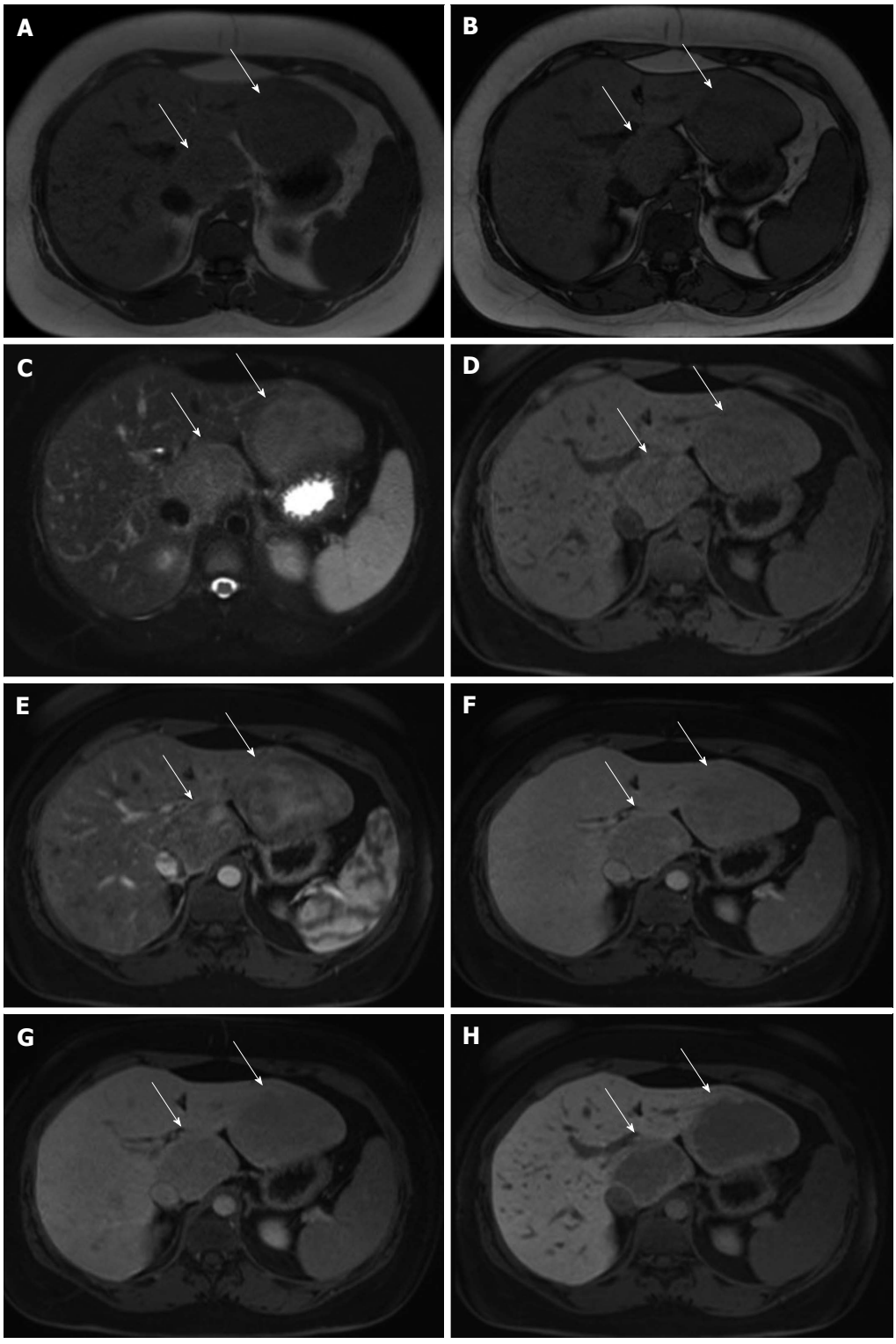

Figure 3 Hepatocellular adenomas. In- (A) and opposed-phase (B) GRE T1-WI, fat-suppressed FSE T2-WI (C), pre (D) and post hepatocyte-specific contrast agent (Eovist®) fat-suppressed 3D-GRE T1-WI at the arterial (E), portal venous (F), interstitial (G) and hepatobiliary (H) phases. Two focal liver lesions are noted on the left and caudate lobes (arrows, A-G) of a noncirrhotic liver, showing slight drop of signal intensity on opposed-phase (B) comparing with the in-phase (A) T1-WI, which is related to minimally fat content. Note that the liver parenchyma also shows minimal steatosis. The lesions demonstrate mild high signal intensity on T2-WI (C), heterogeneous enhancement on the postcontrast arterial phase image (E) and subsequent washout on later postcontrast images (F and G). On the hepatobiliary phase, acquired 20 min after the hepatocyte-specific contrast agent, the lesions show no contrast uptake, excluding the diagnosis of FNHs. GRE: Gradient-echo; FSE: Fast spinecho; T1-WI: T1-weighted images; FNH: Focal nodular hyperplasias.

of the capsule, septa, and any mural nodules[1,55]. Biliary cystadenocarcinoma can develop from a BCA. It can be difficult to differentiate BCA and biliary cystadenocarcinoma preoperatively, but this is usually unnecessary on short-term, as both require complete surgical excision[1,52].

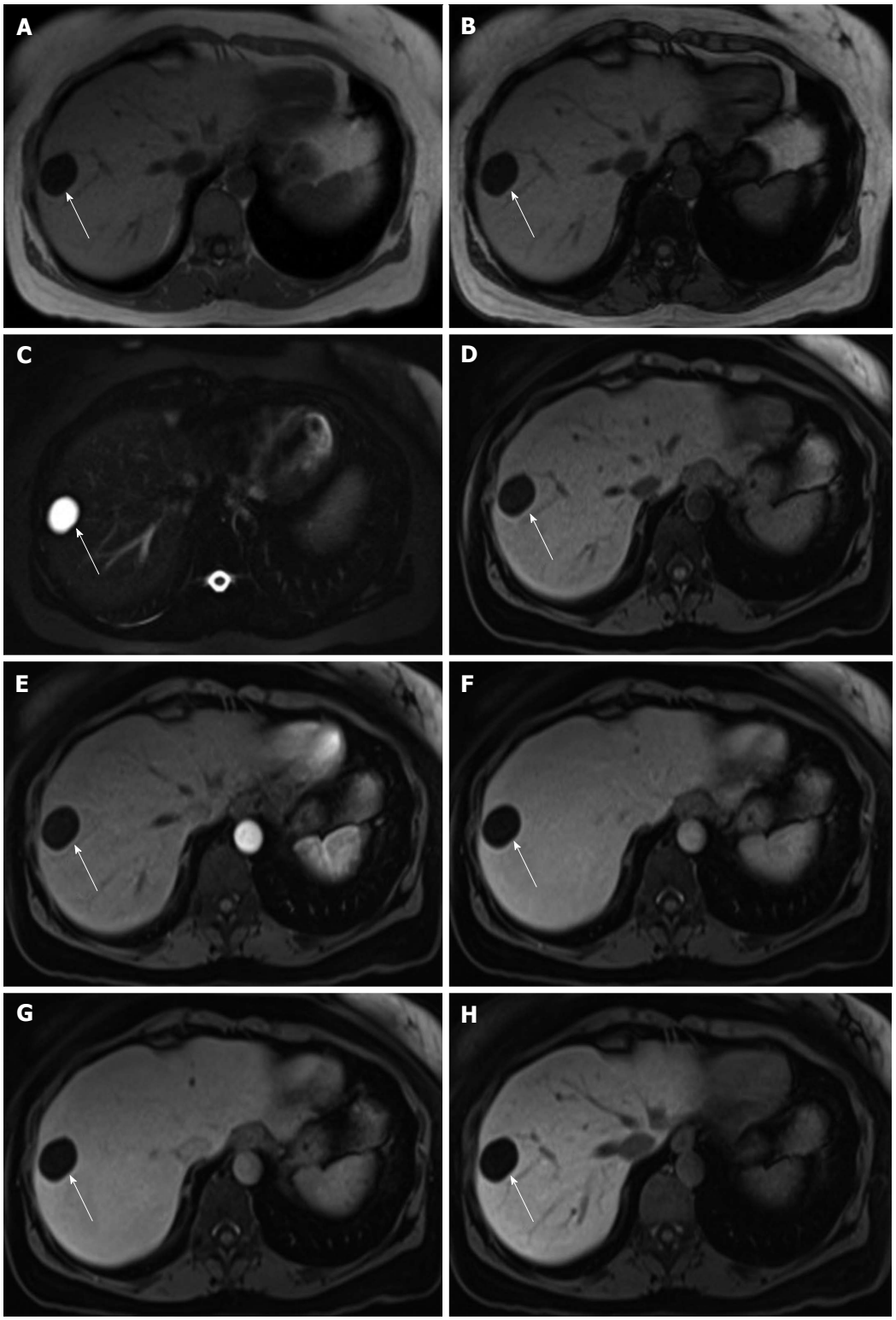

Figure 4 Cyst. In- (A) and opposed-phase (B) GRE T1-WI, fat-suppressed FSE T2-WI (C), pre (D) and post hepatocyte-specific contrast agent (Eovist®) fat-suppressed 3D-GRE T1-WI at the arterial (E), portal venous (F), interstitial (G) and hepatobiliary (H) phases. There is a well-defined lesion on the right hepatic lobe (arrow, A-H) showing marked homogeneous low signal intensity on T1-WI (A, B and D), homogeneous very high signal intensity on T2-WI (C) and no enhancement after gadolinium administration (E-H), consistent with simple liver cyst. GRE: Gradient-echo; FSE: Fast spinecho; T1-WI: T1-weighted images.

MALIGNANT LESIONS

HCC

HCC is a malignant neoplasm with hepatocellular origin. It is the most common primary malignancy of the liver and it occurs almost exclusively in the context of chronic liver disease (CLD) and liver cirrhosis[56]. HCC has been proved to develop by multistep carcinogenesis from a low grade dysplastic nodules to an overt HCC, in a progressive dedifferentiation and neoangiogenesis phenomena[56-58].

MRI plays a pivotal role in the detection and char-

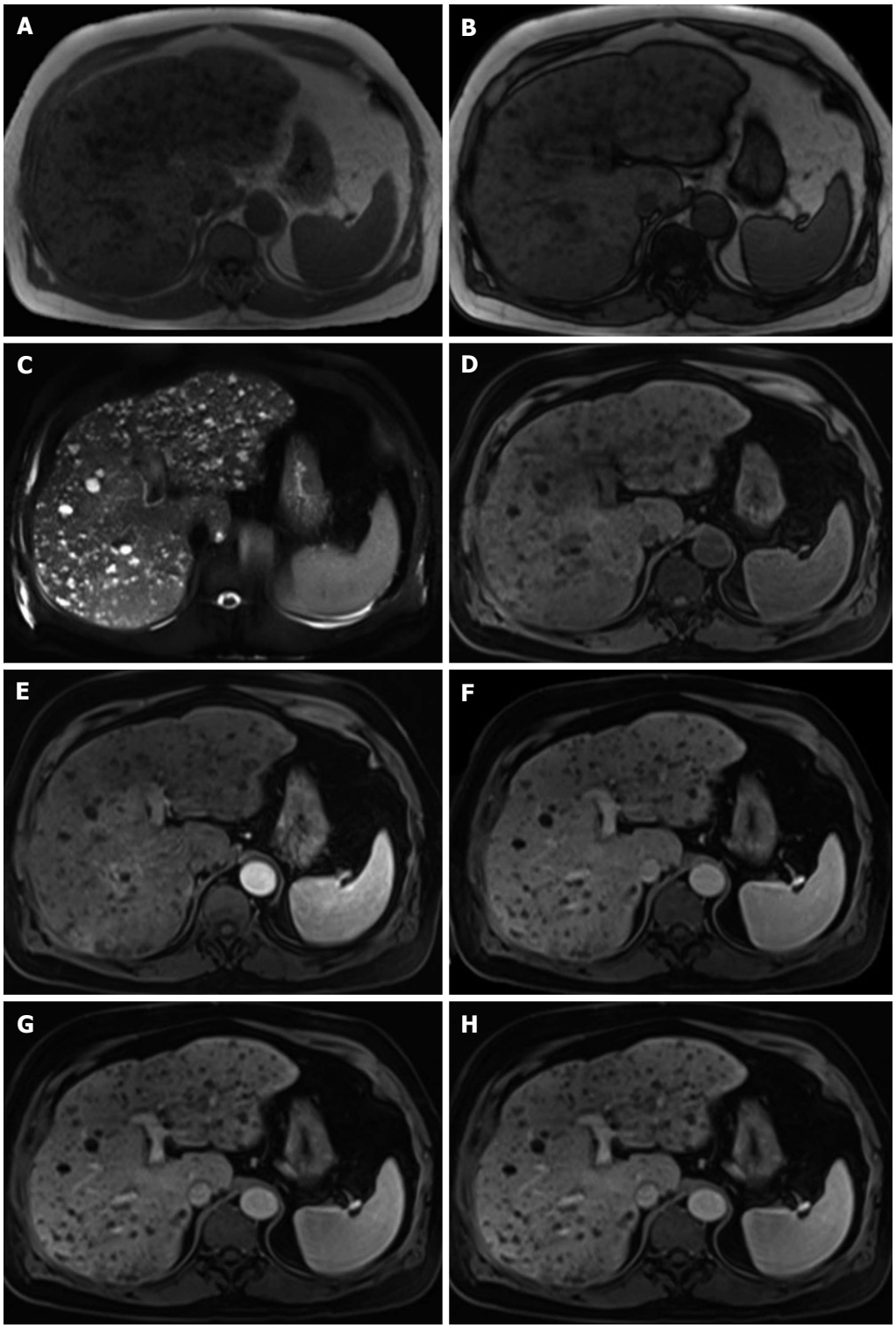

Figure 5 Multiple biliary hamartomas (also known as von Meyenburg complex). In- (A) and opposed-phase (B) GRE T1-WI, fat-suppressed FSE T2-WI (C), pre (D) and postcontrast fat-suppressed 3D-GRE T1-WI at the arterial (E), portal venous (F) and interstitial (G) phases. There are multiple well-defined lesions scattered throughout the liver, smaller than 1.5 cm each. The lesions show low signal intensity on T1-WI (A, B and D), high signal intensity on T2-WI (C) and no enhancement after gadolinium administration (E-G). A thin peripheral enhancement is often present due to compressed liver parenchyma. GRE: Gradient-echo; FSE: Fast spinecho; T1-WI: T1-weighted images.

acterization of HCC, with estimated sensitivity and specificity of 97.4% and 100%, respectively[59,60]. Even for HCC with a size < 2 cm, MRI have a good sensitivity, estimated to 82.6%[60]. This is particularly important since successful treatment of HCC is dependent on early detection and diagnosis[59,61].

In the context of CLD, classic MRI findings of HCC include slightly low signal intensity on T1-WI, slightly high signal intensity on T2-WI, increased heterogeneous arterial enhancement, and washout with fibrous tumor

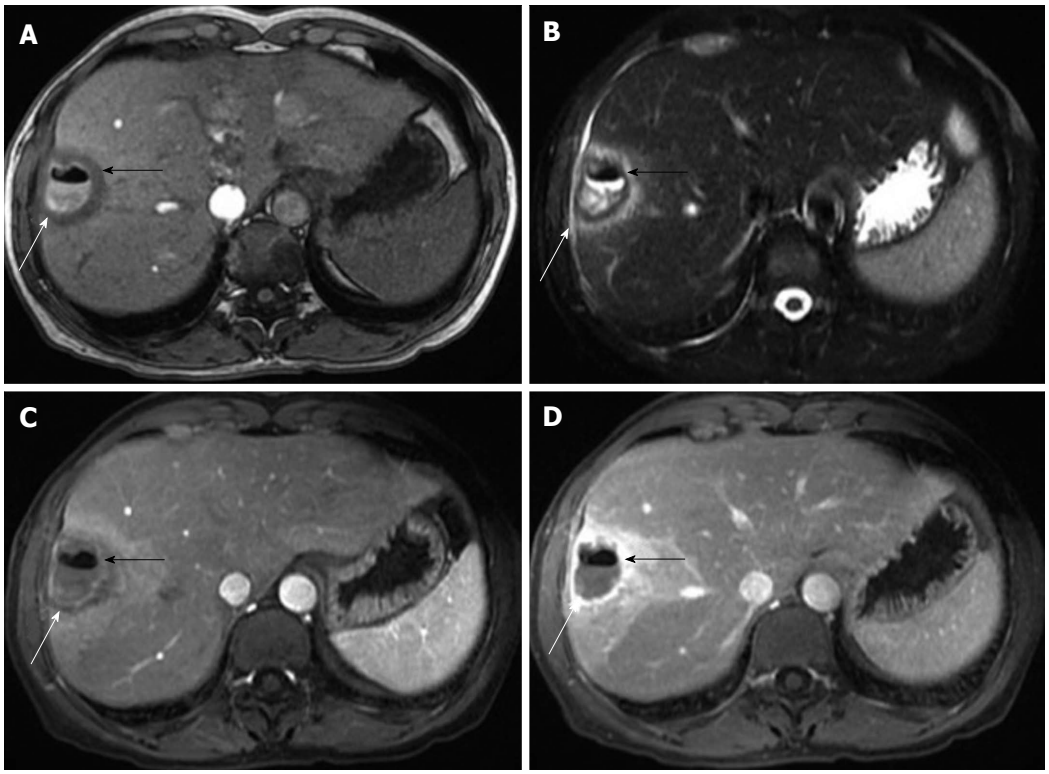

Figure 6 Abscess. GRE T1-WI (A), fat-suppressed FSE T2-WI (B), and postcontrast fat-suppressed 3D-GRE T1-WI at the arterial (C) and portal venous (D) phases. A thick-walled oval shaped lesion is present on the right hepatic lobe (white arrow, A-D), showing an air/fluid level content (black arrow, A-D). There is an associated halo of edema surrounding the lesion, showing low signal intensity on T1-WI (A), high signal intensity on T2-WI (B) and marked enhancement after gadolinium administration (C and D), which is consistent with active inflammation. GRE: Gradient-echo; FSE: Fast spinecho; T1-WI: T1-weighted images.

capsule enhancement on the delayed phase[62] (Figure 7).

The 2011 recommendations by the Association for the Study of Liver Diseases state that a diagnosis of HCC is made if a nodule larger than 1 cm is depicted on MRI (or multi-detector computed tomography), showing arterial enhancement and subsequent "washout" during portal venous or equilibrium phases[63]. These guidelines criteria show a lower sensitivity and specificity for small HCCs (< 2 cm)[64-66]. In order to improve the accuracy of MRI on small HCC, other parameters may be used in conjunction with the dynamic post-contrast sequences, namely high signal on DWI or T2-WI[64,67]. With HSA, most HCC lesions show prominent hypointensity compared to the hyperintense background liver parenchyma because of the absence of normal functional hepatocytes[67]. Although, uncommonly, well-differentiated HCCs may show some enhancement on the hepatobiliary phase[12,68,69]. The combination of routine dynamic and hepatobiliary imaging has been reported to be both sensitive and specific for HCC (sensitivity 67%-97%, specificity 83%-98%)[69,70-77]. Two recent meta-analyses found a pooled sensitivity of 91% and specificity of 93%[78,79].

In the context of CLD and cirrhosis, the distinction between benign and precursor lesions (regenerative and dysplastic nodules, respectively) and HCCs is of the utmost importance[80]. Although they can present with higher T1 signal intensity compared to background liver tissue, regenerative nodules are often indistinct on T1- and T2-WI. The dynamic post-contrast imaging show the same signal as the background parenchyma throughout all phases[12,14]. Dysplastic nodules show histological characteristics of abnormal growth caused by genetic alteration and are classified accordingly to the level of dysplasia, on low- and high-grade dysplastic nodules[14]. On MRI, low-grade dysplastic nodules are often indistinctive from regenerative nodules, and radiologists reserve that terminology for lesions larger than 2 cm in size[12,81]. High-grade dysplastic nodules show iso to high signal on T1-WI and iso signal intensity on T2-WI. They may show intense early enhancement and fade to isointensity, but do not show washout[12,81]. As opposed to HCC, regenerative and low-grade dysplastic nodules show iso-enhancement to the surrounding liver parenchyma. Patients with the diagnosis of high-grade dysplastic nodules are at higher risk of developing HCC and should have closer follow-up MRI.

IHC

IHC is the second most common primary hepatic malignancy, accounting for 10%-20% of all primary liver malignancies[82-84]. Background of CLD such as cholangitis, viral hepatitis (especially hepatitis C) and liver cirrhosis, are known specific risk factors[84]. Primary sclerosing cholangitis is the most well known of these conditions. In terms of growth characteristics, cholangiocarcinomas may be mass-forming, periductal-infiltrating, or

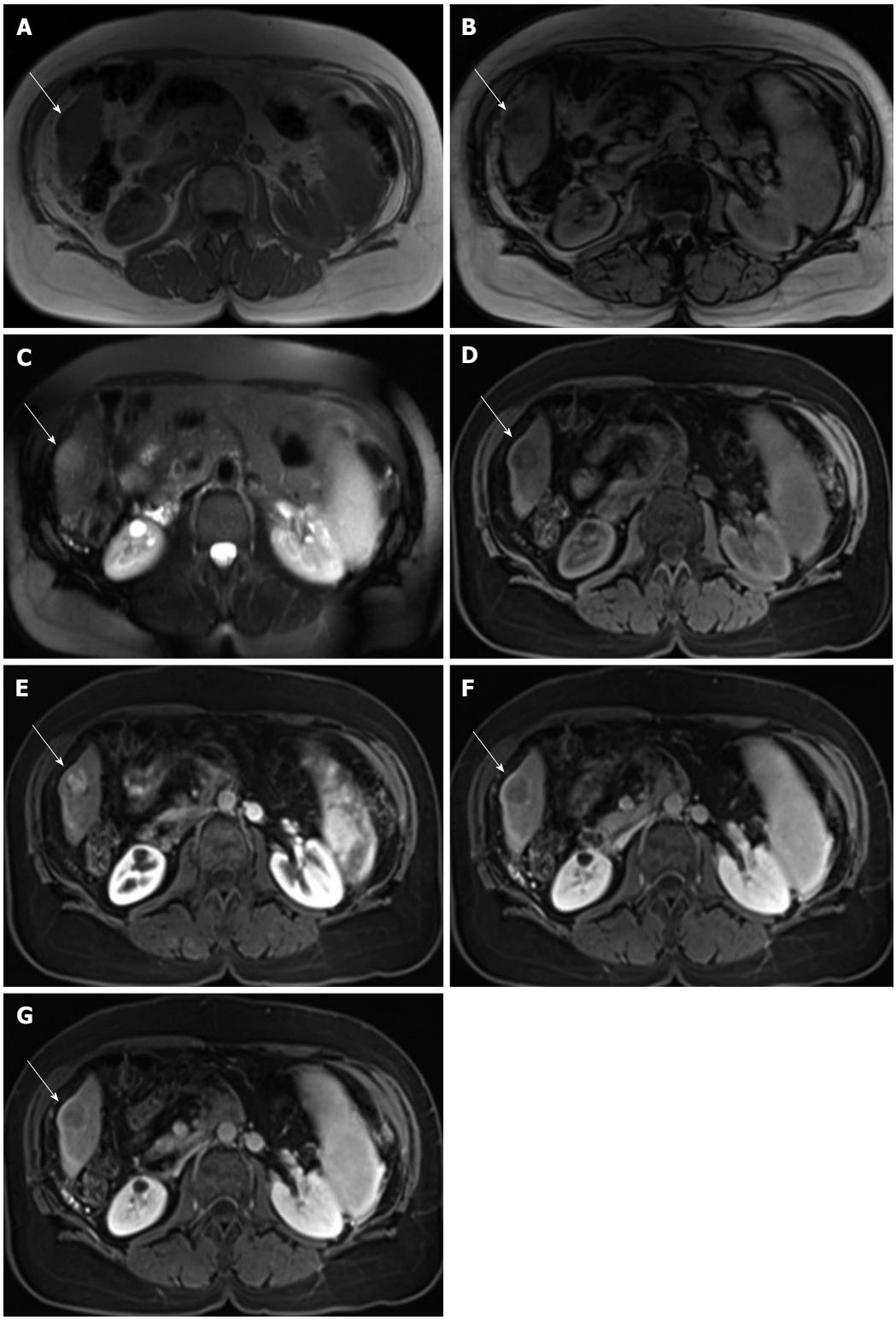

Figure 7 Hepatocellular carcinoma. In- (A) and opposed-phase (B) GRE T1-WI, fat-suppressed FSE T2-WI (C), pre (D) and postcontrast fat-suppressed 3D-GRE T1-WI at the arterial (E), portal venous (F) and interstitial (G) phases. There is a small peripheral lesion on the right lobe of a cirrhotic liver (arrow, A-G), showing drop of signal intensity on opposed-phase (B) comparing with the in-phase (A) images, which is suggestive of fat content. The lesion demonstrates mild high signal intensity on T2-WI (C), low signal intensity on pre-contrast T1-WI (C), heterogeneous enhancement on early post-contrast (E) and subsequent washout with associated pseudocapsule on delayed post-contrast images (F and G), in keeping with a small fat-containing hepatocellular carcinoma. GRE: Gradient-echo; FSE: Fast spinecho; T1-WI: T1-weighted images.

intraductal. Mass-forming cholangiocarcinoma is the most common IHC, accounting for the majority of IHC, and are defined as a rounded mass located in the liver parenchyma[83,84].

MRI allows the distinction between IHC and HCC with high degree of confidence. At present, MRI with

MR cholangiopancreatography has become the imaging modality of choice for diagnosis and staging of cholangiocarcinoma, with the similar accuracy of computed tomography combined with direct cholangiography[85]. The MR appearance of IHC depends on the proportion of fibrosis, necrosis and mucin. Typically they show low to iso-signal intensity on T1-WI, and variably high signal intensity on T2-WI[82,83]. Capsular retraction is sometimes described, reflecting the desmoplastic nature of the tumor. In some cases vascular encasement and dilated bile ducts peripheral to the mass may be seen. Early continuous rim enhancement followed by progressive heterogeneous enhancement of the remainder of the lesion is often seen (Figure 8). The late enhancement is due to the fibrotic nature of cholangiocarcinoma. Near one third of cholangiocarcinomas are hypervascular. Nanashima *et al*[86], Kim *et al*[87] and Al Ansari *et al*[84] reported that 46%, 29%, and 28%, respectively, of the intra-hepatic cholangiocarcinomas in their studies showed hypervascular enhancement pattern. This appearance is well recognized and might carry a better prognosis with longer disease-free survival[87,88]. Conversely, IHC in patients with chronic viral hepatitis or cirrhosis tend to be very hypervascular[86,89]. Xu *et al*[90] showed that the density of arteries and micro-vessels of IHC in a cirrhotic liver was higher than that in IHC without underlying cirrhosis and comparable to that in cholangiocarcinoma component of combined HCC-IHC. This vascular difference in IHC may be responsible for the hypervascular enhancement of IHC in the context of cirrhosis[90].

When using HSA, mass-forming IHC may have a pseudowashout pattern with Eovist®-enhanced MR images because of progressive background liver enhancement and no enhancement of the IHC[91]. Hepatobiliary imaging with Eovist®, showed increased lesion conspicuity and better delineation of secondary nodules and intrahepatic metastasis, which may aid the evaluation of IHC[92]. Further, it has been suggested that it can be helpful for therapy planning due to the exact depiction of the tumor borders[93].

Satellite lesions are markedly more conspicuous on hepatobiliary phase of Eovist®-enhanced MRI, proposing a potential role for hepatobiliary MR agents in evaluation of the tumor resectability. In a study by Kim *et al*[87], 93% of mass-forming intra-hepatic cholangiocarcinoma exhibited a special pattern of enhancement in hepatobiliary phase of Eovist®-enhanced MRI, described as cloud-like hyperintensity in the central portion of the tumors, surrounded with a low signal intensity rim, which appears as a defect in the vicinity of the hyperintense normal liver parenchyma.

Metastasis

Metastasis is the most common liver malignancy, outnumbering primary liver malignant neoplasms with a ratio of 40:1. Moreover, it has been shown that 40% of patients with extrahepatic malignancy show liver metastasis at the autopsy. Accurate detection and characterization of liver metastasis is critical in patient management, namely in determining treatment and prognosis[26]. MR is rapidly evolving as the primary imaging modality for the detection and characterization of liver lesions including metastases in many centers.

On MRI, hepatic metastases have variable appearances depending on the primary tumor. Generally, metastases show mild to moderate high signal intensity on T2-WI and low signal intensity on precontrast T1-WI. Cystic metastases and those with necrosis show increased T2 signal (more common in neuroendocrine tumors, sarcomas, and melanoma metastases). A subset of liver metastases shows T1 hyperintensity for a variety of reasons. One subset is the fat-containing metastases, which are easily characterized by the drop of signal on OP and/or fat-suppressed sequences. Other subset is metastases that contain paramagnetic substances such as melanin, extracellular methemoglobin and protein. A good example is melanoma metastases, which are often T1 hyperintense because of their melanocytic content and/or occasional hemorrhage. On dynamic post-contrast imaging, metastases are characterized as hypervascular, iso-vascular, or hypovascular, when they show more, similar, or less enhancement compared to the background liver parenchyma, respectively, at the late arterial hepatic dominant phase (Figure 9).

Most of liver metastases are from extra-hepatic adenocarcinomas and generally they tend to be hypovascular[82]. Hypervascular metastases are usually seen in neuroendocrine tumors, renal cell, thyroid and breast carcinoma, melanoma, and sarcoma.

HSAs and DWI are useful for detection of small hepatic metastases, demonstrating improved sensitivity over conventional T2-WI MR techniques and, significantly increased sensitivity compared to CT imaging[27,94-96]. As metastatic tumors do not contain functioning hepatocytes, they appear hypointense during the hepatocellular phase, resulting in a high contrast between enhancing liver tissue and metastases[26]. Metastases show high signal on DWI and may increase the confidence of the diagnosis[94,95]. The combination of HSAs and DWI yield better diagnostic accuracy and sensitivity in the detection of small liver metastasis than each magnetic resonance scan sequence alone. In one study, the combined set showed significantly improved sensitivity (mean values, 97.5%/95.0% on per-lesion/per-patient basis) than each imaging set alone (mean, 90.7%/83.7% for Eovist® set, and 91.6%/83.0% for DWI set) on both per-lesion basis and per-patient basis[97].

While the use of MRI on detection and characterization of liver metastatic disease is well established, the role on the assessment of treatment response is less defined[21]. It has been suggested the benefits of MRI over CT[98-100]. This is evident in the setting of pseudoprogression diagnosed on CT due to high density of hemorrhagic treated lesions and bevacizumab-containing chemotherapy regimens on metastatic colorectal cancer[98-100]. However, more studies are needed in order

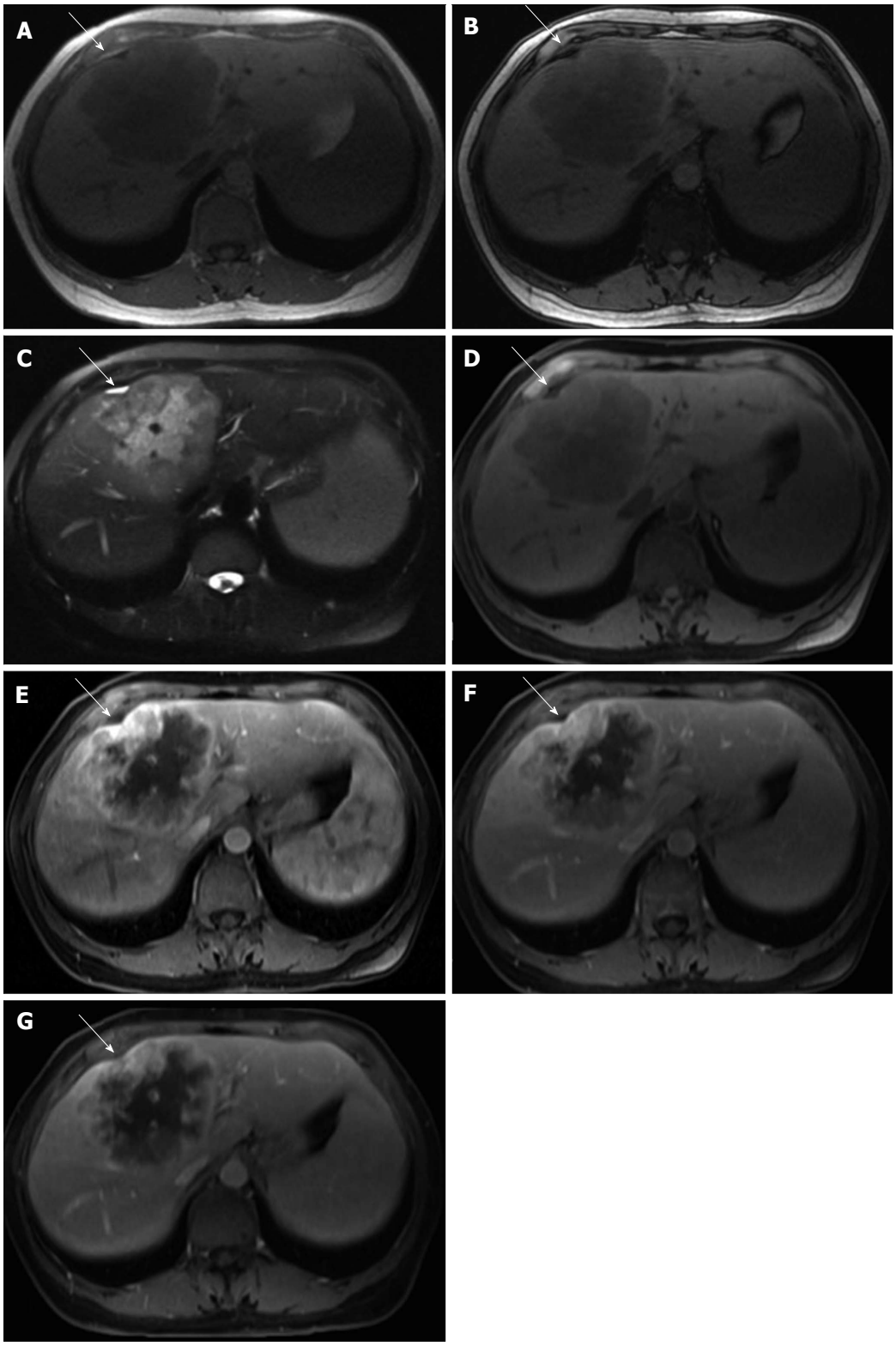

Figure 8 Intrahepatic cholangiocarcinoma. In- (A) and opposed-phase (B) GRE T1-WI, fat-suppressed FSE T2-WI (C), pre (D) and postcontrast fat-suppressed 3D-GRE T1-WI at the arterial (E), portal venous (F) and interstitial (G) phases. The tumor shows low signal intensity on T1-WI (A, B and D), high signal intensity on T2-WI (C), and heterogeneous peripheral continuous and progressive enhancement on postgadolinium images (E-G). Associated capsular retraction is also noted (white arrow, A-G). GRE: Gradient-echo; FSE: Fast spinecho; T1-WI: T1-weighted images.

to fully comprehend the role of MRI on the assessment of treatment response of metastatic liver lesions.

Simplified practical approach

MRI is a highly sensitive and accurate modality for the characterization of FLL. Although many hepatic lesions have characteristic imaging features, the interpretation should rely on a combination of lesion assessment, background liver assessment, and clinical parameters. For liver lesion characterization, HSA are

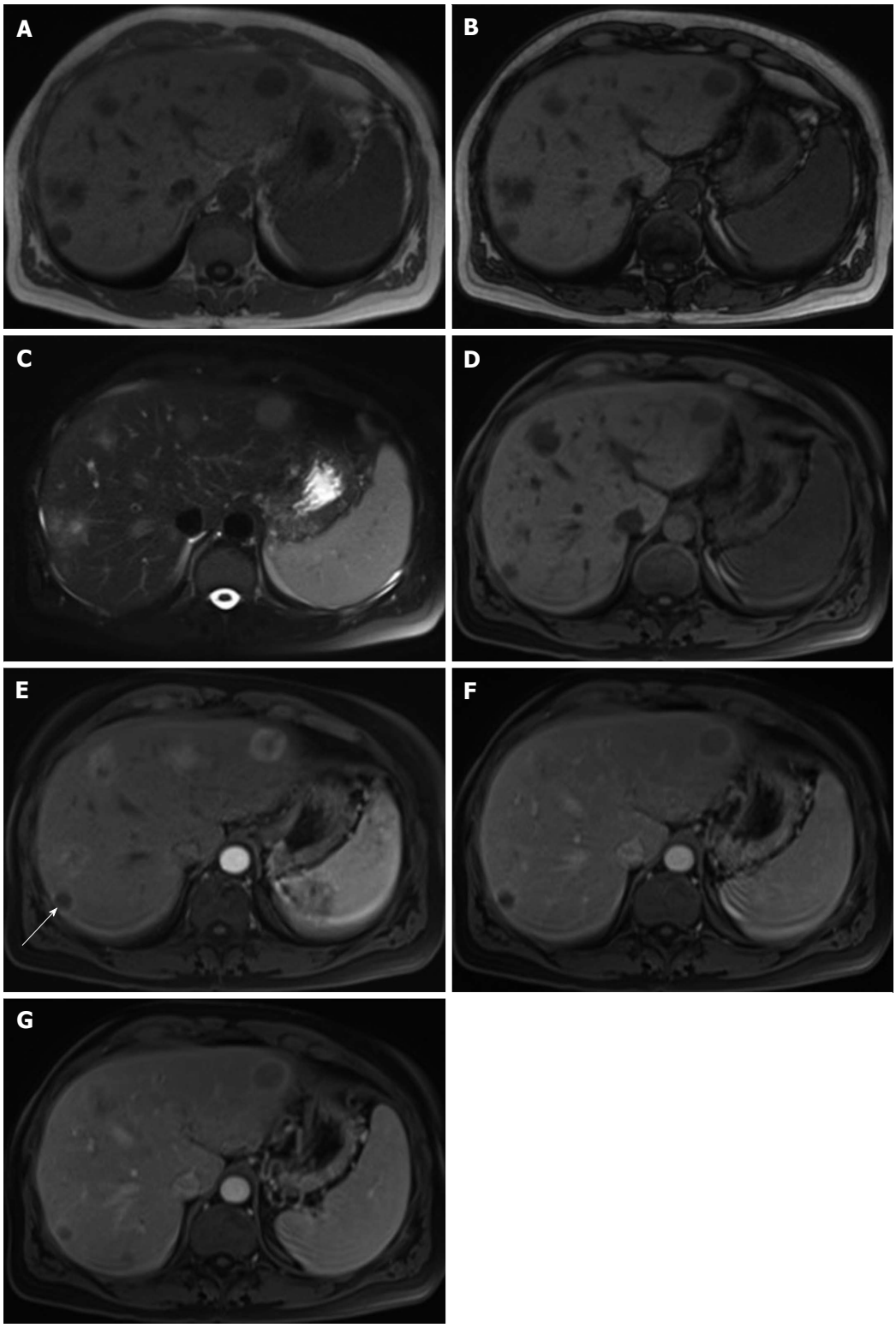

Figure 9 Metastases. In- (A) and opposed-phase (B) GRE T1-WI, fat-suppressed FSE T2-WI (C), pre (D) and postcontrast fat-suppressed 3D-GRE T1-WI at the arterial (E), portal venous (F) and interstitial (G) phases. Multiple metastases are present throughout the liver, showing low signal intensity on T1-WI (A, B and D) and high signal intensity on T2-WI. Most of these lesions show hypervascular characteristics, while one in segment VII (arrow, E) shows ring enhancement. Late washout is perceived, a feature that is characteristic of carcinoid metastases (G). GRE: Gradient-echo; FSE: Fast spinecho; T1-WI: T1-weighted images.

used to assess the presence of intralesional functional hepatocytes. DWI is also useful in differentiating benign from malignant lesions. Although clinical utility has been proven, further investigation is needed to better delineate the role of HSA and DWI in characterizing FLL. A simplified schematic representation of the typical imaging features of the most common benign and malignant hepatic lesions is provided in Figures 10 and 11.

The hepatocellular nature of a lesion can usually

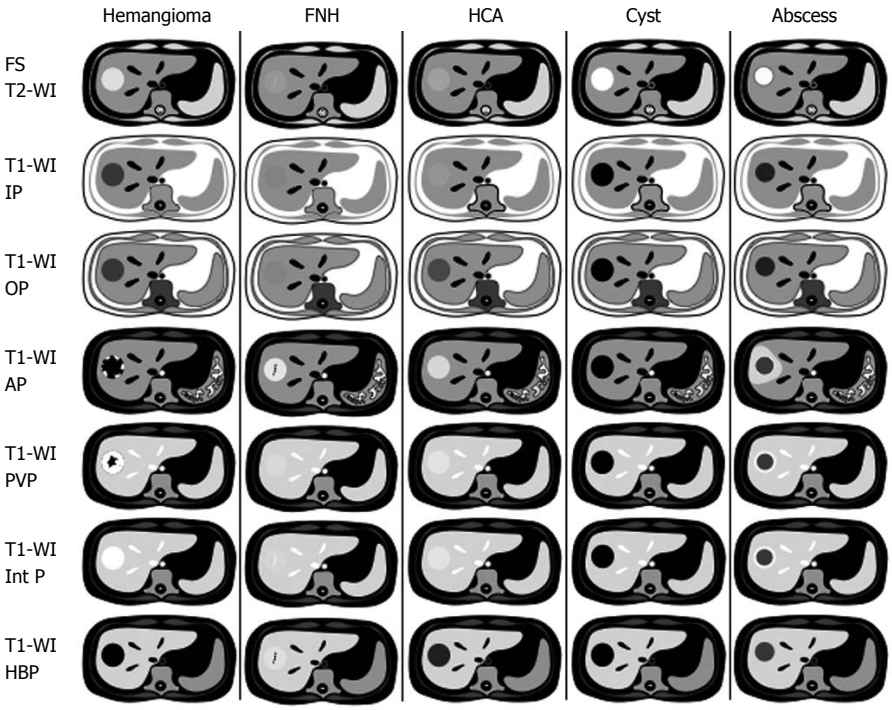

Figure 10 Stereotypical simplified schema, showing magnetic resonance imaging features of benign focal liver lesions. FNH: Focal nodular hyperplasia; HCA: Hepatocellular adenoma; FS T2-WI: Fat-suppressed T2-weighted image; T1-WI IP: T1-weighted in-phase image; T1-WI OP: T1-weighted out-of-phase image; T1-WI AP: Post-contrast fat-suppressed T1-weighted image at the late arterial phase; T1-WI PVP: Post-contrast fat-suppressed T1-weighted image at the portal-venous phase; T1-WI Inter P: Post-contrast fat-suppressed T1-weighted image at the interstitial phase; T1-WI HBP: Post-contrast fat-suppressed T1-weighted image at the hepatobiliary phase (with hepatocyte-specific contrast agent).

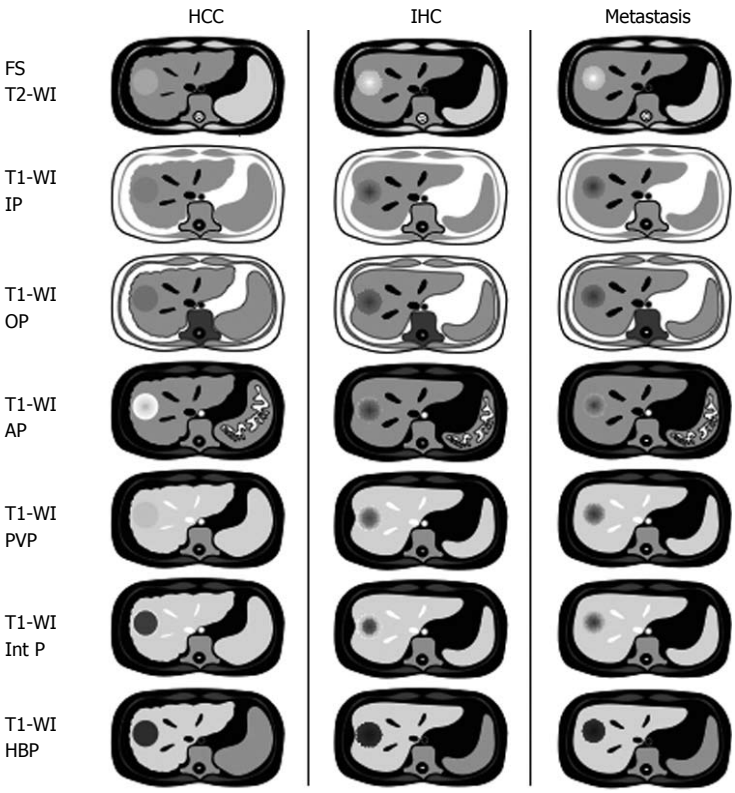

Figure 11 Stereotypical simplified schema, showing magnetic resonance imaging features of malignant focal liver lesions. The represented metastasis exemplifies the typical appearance of a hypovascular metastasis (the most common type). FS T2-WI: Fat-suppressed T2-weighted image; T1-WI IP: T1-weighted in-phase image; T1-WI OP: T1-weighted out-of-phase image; T1-WI AP: Post-contrast fat-suppressed T1-weighted image at the late arterial phase; T1-WI PVP: Post-contrast fat-suppressed T1-weighted image at the portal-venous phase; T1-WI Inter P: Post-contrast fat-suppressed T1-weighted image at the interstitial phase; T1-WI HBP: Post-contrast fat-suppressed T1-weighted image at the hepatobiliary phase (with hepatocyte-specific contrast agent); HCC: Hepatocellular carcinomas; IHC: Intrahepatic cholangiocarcinomas.

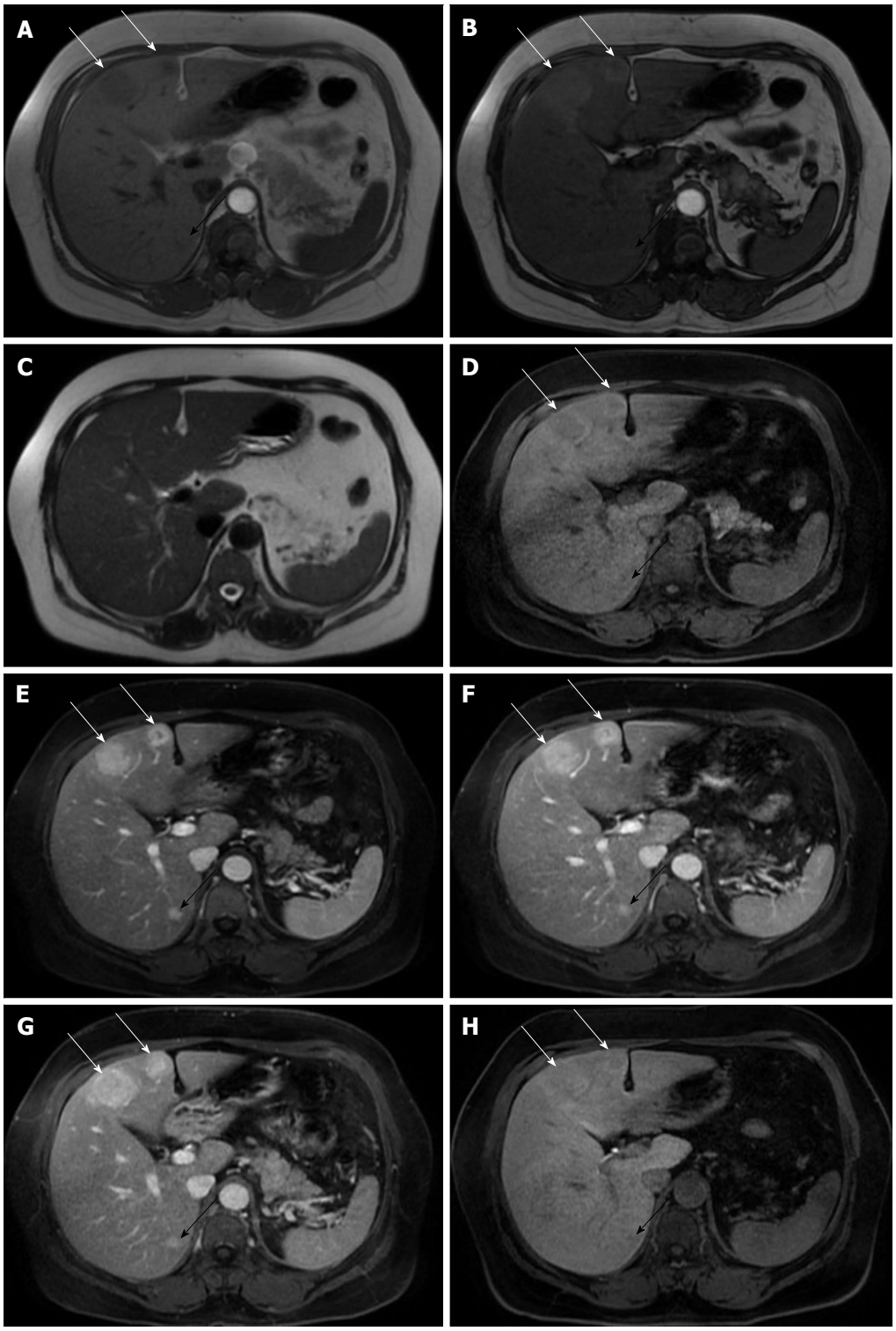

Figure 12 Multiple focal nodular hyperplasias. In- (A) and opposed-phase (B) GRE T1-WI, fat-suppressed FSE T2-WI (C), pre (D) and post hepatocyte-specific contrast agent (Eovist®) fat-suppressed 3D-GRE T1-WI at the arterial (E), portal venous (F), interstitial (G) and hepatobiliary (H) phases. There are two focal nodular hyperplasias on the left lobe (white arrows) and one small FNH on the right lobe (black arrow). The liver parenchyma shows drop of signal in the opposed-phase (B) comparing to the in-phase images (A), indicating moderate parenchymal fat deposition. Note that the lesions do not show drop in signal in the opposed-phase (B). All lesions are isointense comparing to the surrounding liver on T2-WI (C), showing uniform blush on the early post-contrast images (E). In this case the lesions enhancement do not fade to isointensity on the delayed post-contrast images (F and G) due to the presence of moderate fat deposition in the liver parenchyma. On the hepatobiliary phase, 20 min after the administration the hepatocyte-specific contrast agent, the lesions show uptake of the contrast agent. GRE: Gradient-echo; FSE: Fast spinecho; T1-WI: T1-weighted images.

be assessed by the unenhanced sequences. The signal intensity of these lesions is similar to the liver parenchyma. The multi-phasic dynamic post-contrast imaging further helps in characterization, while HSA may differentiate between normal or abnormal hepatocyte function.

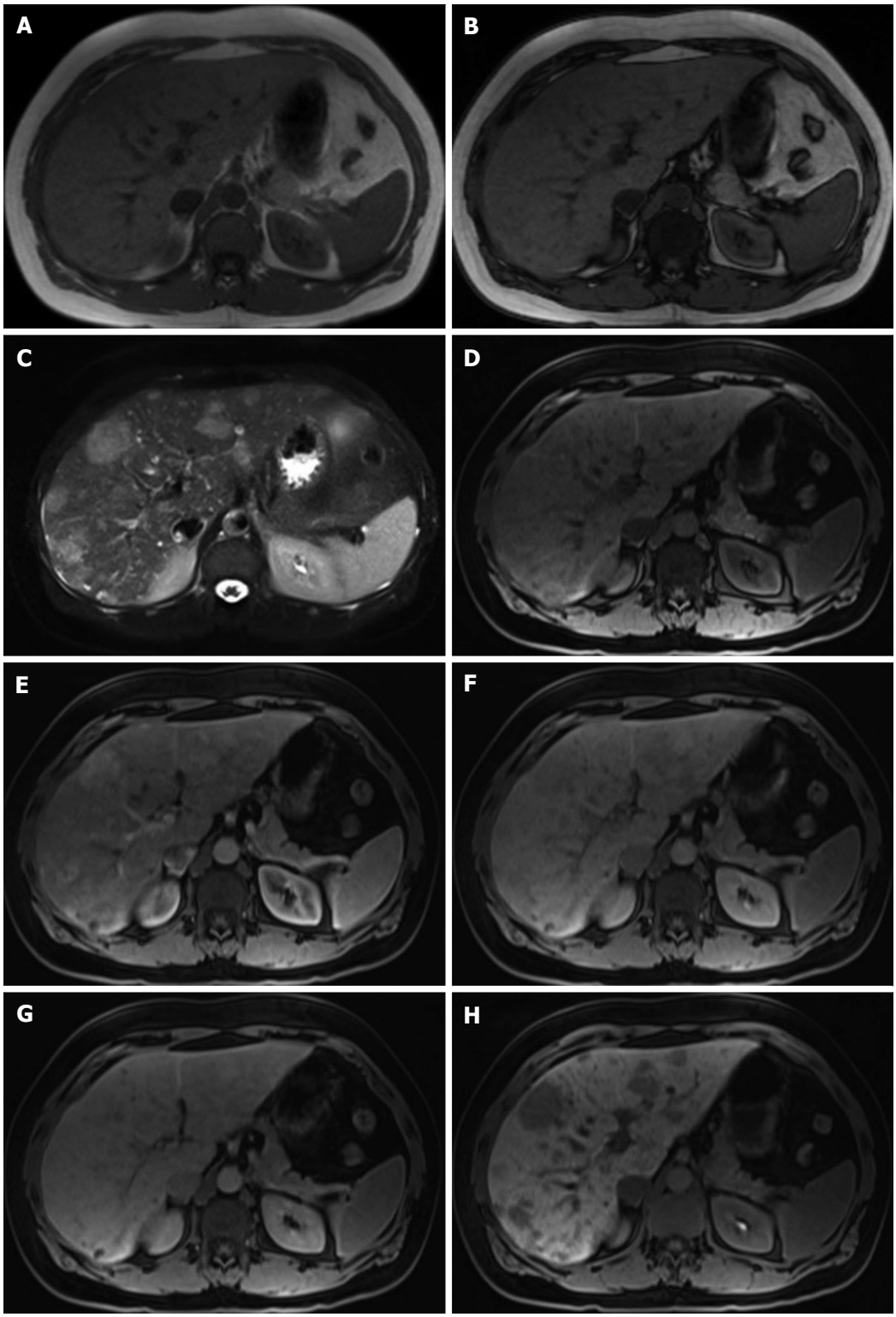

Figure 13 Adenomatosis. In- (A) and opposed-phase (B) GRE T1-WI, fat-suppressed FSE T2-WI (C), pre (D) and post hepatocyte-specific contrast agent (Eovist®) fat-suppressed 3D-GRE T1-WI at the arterial (E), portal venous (F), interstitial (G) and hepatobiliary (H) phases. There are multiple lesions (> 10 in number) scattered throughout the hepatic parenchyma, barely visible on unenhanced T1-WI (A, B and D) and hyperintense on T2-WI (C). The lesions show arterial enhancement (E), which fades to almost isointensity on the delayed post-contrast images (F and G). On the hepatobiliary phase, acquired 20 min after the hepatocyte-specific contrast agent, all lesions appear with low signal intensity comparing to the surrounding liver. GRE: Gradient-echo; FSE: Fast spinecho; T1-WI: T1-weighted images.

Although prone to restraint, an exercise of a simplistic approach taking into consideration the clinical information and the MR findings can be performed. In young women, a nodular liver lesion that looks similar in signal to the remaining parenchyma on unenhanced MR (suggesting hepatocellular origin), and showing strong enhancement on the late arterial phase, the diagnosis of FNH, or less likely, HCA should be considered. MRI

with HSA usually allows the distinction between these two lesions.

Hemangiomas usually display pathognomonic imaging features, namely the moderately high signal intensity on T2-WI and the peripheral globular discontinuous enhancement and retention of contrast on delayed images. Furthermore, in a patient without underlying liver disease or history of extra-hepatic cancer, a lesion with moderately high signal intensity on T2-WI that strongly enhances at the arterial phase and remains high in signal intensity on subsequent phases is also typical of capillary liver hemangioma. As mentioned above, while using Eovist®, one should remind that hemangiomas can show "pseudowashout", simulating malignant lesions.

In patients with multiple liver tumors, different types of lesions frequently occur in particular combinations. The most frequent combination is hemangioma and FNH, which occurs in near 25% of patients. Less frequently, FNH and hepatocellular adenoma may present as multiple lesions and typically show similar characteristics of singular lesions (Figure 12). Liver adenomatosis (> 10 adenomas), is an uncommon entity that occurs most often in young women and has three MRI patterns that are associated with three pathologic forms as described above[101] (Figure 13).

In patients with underlying liver disease regenerative hepatocellular nodules, dysplastic nodules, and HCCs are by far the most common lesions. In this setting, a nodular liver lesion that looks similar in signal to the liver parenchyma on unenhanced MR (hepatocellular origin), and shows enhancement similar to the background liver parenchyma throughout all phases are regenerative or low-grade dysplastic nodules; if they show hyper-enhancement but no washout, they are regarded as high-grade dysplastic nodules; and if they show hyper-enhancement and delayed washout, then the diagnosis of HCC is established. Ancillary findings of mildly high T2 signal intensity or restriction on diffusion in case of hypervascular nodules, despite the presence of washout, is also very suspicious for HCC.

Although the prevalence of benign lesions in patients with cancer remains high, one should always consider the possibility of liver metastases, especially when liver lesions are small and cannot be fully characterized by other imaging methods such as CT. Multiple solid liver lesions that do not show pathognomonic appearance of any of the common benign liver lesion in a patient with a known history of extra-hepatic malignancy are very suspicious for liver metastases.

CONCLUSION

Different imaging sets can be obtained in a single MRI examination, reflecting a greater range of chemical and physical properties of both normal and abnormal tissue. MRI is capable of providing comprehensive and highly accurate diagnostic information, with the additional advantage of lack of harmful ionizing radiation. These properties make MRI the mainstay for the noninvasive evaluation of focal liver lesions. Like with other radiologic exams, the interpretation of a liver MR should be done in a by-patient fashion. The expertise of an experienced subspecialized abdominal MR radiologist is paramount to establish and maintain high-quality liver MR protocols, determine the appropriate indications for the utilization of hepatocyte *vs* extracellular contrast agents, and interpret MR studies; therefore, consistently yielding a correct diagnosis and ultimately setting the right path and pace for patients' management.

REFERENCES

1 **Cogley JR**, Miller FH. MR imaging of benign focal liver lesions. *Radiol Clin North Am* 2014; **52**: 657-682 [PMID: 24889166 DOI: 10.1016/j.rcl.2014.02.005]

2 **Ramalho M**, de Campos RO, Heredia V, Dale BM, Tannaphai P, Azevedo RM, Semelka RC. Characterization of adrenal lesions with 1.5-T MRI: preliminary observations on comparison of three in-phase and out-of-phase gradient-echo techniques. *AJR Am J Roentgenol* 2011; **197**: 415-423 [PMID: 21785088 DOI: 10.2214/AJR.10.5848]

3 **Ronot M**, Bahrami S, Calderaro J, Valla DC, Bedossa P, Belghiti J, Vilgrain V, Paradis V. Hepatocellular adenomas: accuracy of magnetic resonance imaging and liver biopsy in subtype classification. *Hepatology* 2011; **53**: 1182-1191 [PMID: 21480324 DOI: 10.1002/hep.24147]

4 **Grazioli L**, Bondioni MP, Haradome H, Motosugi U, Tinti R, Frittoli B, Gambarini S, Donato F, Colagrande S. Hepatocellular adenoma and focal nodular hyperplasia: value of gadoxetic acid-enhanced MR imaging in differential diagnosis. *Radiology* 2012; **262**: 520-529 [PMID: 22282184 DOI: 10.1148/radiol.11101742/-/DC1]

5 **Nault JC**, Bioulac-Sage P, Zucman-Rossi J. Hepatocellular benign tumors-from molecular classification to personalized clinical care. *Gastroenterology* 2013; **144**: 888-902 [PMID: 23485860 DOI: 10.1053/j.gastro.2013.02.032]

6 **Bastati N**, Feier D, Wibmer A, Traussnigg S, Balassy C, Tamandl D, Einspieler H, Wrba F, Trauner M, Herold C, Ba-Ssalamah A. Noninvasive differentiation of simple steatosis and steatohepatitis by using gadoxetic acid-enhanced MR imaging in patients with nonalcoholic fatty liver disease: a proof-of-concept study. *Radiology* 2014; **271**: 739-747 [PMID: 24576046 DOI: 10.1148/radiol.14131890]

7 **Fowler KJ**, Brown JJ, Narra VR. Magnetic resonance imaging of focal liver lesions: approach to imaging diagnosis. *Hepatology* 2011; **54**: 2227-2237 [PMID: 21932400 DOI: 10.1002/hep.24679]

8 **Noone TC**, Semelka RC, Chaney DM, Reinhold C. Abdominal imaging studies: comparison of diagnostic accuracies resulting from ultrasound, computed tomography, and magnetic resonance imaging in the same individual. *Magn Reson Imaging* 2004; **22**: 19-24 [PMID: 14972390 DOI: 10.1016/j.mri.2003.01.001]

9 **Taouli B**, Thakur RK, Mannelli L, Babb JS, Kim S, Hecht EM, Lee VS, Israel GM. Renal lesions: characterization with diffusion-weighted imaging versus contrast-enhanced MR imaging. *Radiology* 2009; **251**: 398-407 [PMID: 19276322 DOI: 10.1148/radiol.2512080880]

10 **Garrett R**. Solid liver masses: approach to management from the standpoint of a radiologist. *Curr Gastroenterol Rep* 2013; **15**: 359 [PMID: 24243519 DOI: 10.1007/s11894-013-0359-8]

11 **Vargas HA**, Chaim J, Lefkowitz RA, Lakhman Y, Zheng J, Moskowitz CS, Sohn MJ, Schwartz LH, Russo P, Akin O. Renal cortical tumors: use of multiphasic contrast-enhanced MR imaging to differentiate benign and malignant histologic subtypes. *Radiology* 2012; **264**: 779-788 [PMID: 22829683 DOI: 10.1148/radiol.12110746]

12 **Watanabe A**, Ramalho M, AlObaidy M, Kim HJ, Velloni FG, Semelka RC. Magnetic resonance imaging of the cirrhotic liver:

An update. *World J Hepatol* 2015; **7**: 468-487 [PMID: 25848471 DOI: 10.4254/wjh.v7.i3.468]
13 **Belghiti J**, Cauchy F, Paradis V, Vilgrain V. Diagnosis and management of solid benign liver lesions. *Nat Rev Gastroenterol Hepatol* 2014; **11**: 737-749 [PMID: 25178878 DOI: 10.1038/nrgastro.2014.151]
14 **van den Bos IC**, Hussain SM, de Man RA, Zondervan PE, Ijzermans JN, Preda A, Krestin GP. Magnetic resonance imaging of liver lesions: exceptions and atypical lesions. *Curr Probl Diagn Radiol* 2008; **37**: 95-103 [PMID: 18436109 DOI: 10.1067/j.cpradiol.2007.07.002]
15 **Strassburg CP**, Manns MP. Approaches to liver biopsy techniques--revisited. *Semin Liver Dis* 2006; **26**: 318-327 [PMID: 17051446 DOI: 10.1055/s-2006-951599]
16 **Padia SA**, Baker ME, Schaeffer CJ, Remer EM, Obuchowski NA, Winans C, Herts BR. Safety and efficacy of sonographic-guided random real-time core needle biopsy of the liver. *J Clin Ultrasound* 2009; **37**: 138-143 [PMID: 19184991 DOI: 10.1002/jcu.20553]
17 **Thampanitchawong P**, Piratvisuth T. Liver biopsy: complications and risk factors. *World J Gastroenterol* 1999; **5**: 301-304 [PMID: 11819452]
18 **Lee YJ**, Lee JM, Lee JS, Lee HY, Park BH, Kim YH, Han JK, Choi BI. Hepatocellular carcinoma: diagnostic performance of multidetector CT and MR imaging-a systematic review and meta-analysis. *Radiology* 2015; **275**: 97-109 [PMID: 25559230 DOI: 10.1148/radiol.14140690]
19 **Bartolozzi C**. MR of the liver: from breakthrough to clinical application. *Abdom Imaging* 2012; **37**: 154 [PMID: 21710173 DOI: 10.1007/s00261-011-9773-2]
20 **Acay MB**, Bayramoğlu S, Acay A. The sensitivity of MR colonography using dark lumen technique for detection of colonic lesions. *Turk J Gastroenterol* 2014; **25**: 271-278 [PMID: 25141315 DOI: 10.5152/tjg.2014.4850]
21 **Tirumani SH**, Kim KW, Nishino M, Howard SA, Krajewski KM, Jagannathan JP, Cleary JM, Ramaiya NH, Shinagare AB. Update on the role of imaging in management of metastatic colorectal cancer. *Radiographics* 2014; **34**: 1908-1928 [PMID: 25384292 DOI: 10.1148/rg.347130090]
22 **Xie L**, Guang Y, Ding H, Cai A, Huang Y. Diagnostic value of contrast-enhanced ultrasound, computed tomography and magnetic resonance imaging for focal liver lesions: a meta-analysis. *Ultrasound Med Biol* 2011; **37**: 854-861 [PMID: 21531500 DOI: 10.1016/j.ultrasmedbio.2011.03.006]
23 **Ramalho M**, Altun E, Herédia V, Zapparoli M, Semelka R. Liver MR imaging: 1.5T versus 3T. *Magn Reson Imaging Clin N Am* 2007; **15**: 321-347, vi [PMID: 17893053 DOI: 10.1016/j.mric.2007.06.003]
24 **Goncalves Neto JA**, Altun E, Vaidean G, Elazzazi M, Troy J, Ramachandran S, Semelka RC. Early contrast enhancement of the liver: exact description of subphases using MRI. *Magn Reson Imaging* 2009; **27**: 792-800 [PMID: 19121908 DOI: 10.1016/j.mri.2008.11.003]
25 **Sharma P**, Kalb B, Kitajima HD, Salman KN, Burrow B, Ray GL, Martin DR. Optimization of single injection liver arterial phase gadolinium enhanced MRI using bolus track real-time imaging. *J Magn Reson Imaging* 2011; **33**: 110-118 [PMID: 21182128 DOI: 10.1002/jmri.22200]
26 **Thian YL**, Riddell AM, Koh DM. Liver-specific agents for contrast-enhanced MRI: role in oncological imaging. *Cancer Imaging* 2013; **13**: 567-579 [PMID: 24434892 DOI: 10.1102/1470-7330.2013.0050]
27 **Schwope RB**, May LA, Reiter MJ, Lisanti CJ, Margolis DJ. Gadoxetic acid: pearls and pitfalls. *Abdom Imaging* 2015; Epub ahead of print [PMID: 25613332 DOI: 10.1007/s00261-015-0354-7]
28 **Goodwin MD**, Dobson JE, Sirlin CB, Lim BG, Stella DL. Diagnostic challenges and pitfalls in MR imaging with hepatocyte-specific contrast agents. *Radiographics* 2011; **31**: 1547-1568 [PMID: 21997981 DOI: 10.1148/rg.316115528]
29 **Sandrasegaran K**, Akisik FM, Lin C, Tahir B, Rajan J, Aisen AM. The value of diffusion-weighted imaging in characterizing focal liver masses. *Acad Radiol* 2009; **16**: 1208-1214 [PMID: 19608435 DOI: 10.1016/j.acra.2009.05.013]
30 **Taouli B**, Koh DM. Diffusion-weighted MR imaging of the liver. *Radiology* 2010; **254**: 47-66 [PMID: 20032142 DOI: 10.1148/radiol.09090021]
31 **Culverwell AD**, Sheridan MB, Guthrie JA, Scarsbrook AF. Diffusion-weighted MRI of the liver-Interpretative pearls and pitfalls. *Clin Radiol* 2013; **68**: 406-414 [PMID: 22981728 DOI: 10.1016/j.crad.2012.08.008]
32 **Galea N**, Cantisani V, Taouli B. Liver lesion detection and characterization: role of diffusion-weighted imaging. *J Magn Reson Imaging* 2013; **37**: 1260-1276 [PMID: 23712841 DOI: 10.1002/jmri.23947]
33 **Altun E**, Semelka RC, Dale BM, Elias J. Water excitation MPRAGE: an alternative sequence for postcontrast imaging of the abdomen in noncooperative patients at 1.5 Tesla and 3.0 Tesla MRI. *J Magn Reson Imaging* 2008; **27**: 1146-1154 [PMID: 18425826 DOI: 10.1002/jmri.21346]
34 **Ferreira A**, Ramalho M, de Campos RO, Heredia V, Azevedo RM, Dale B, Semelka RC. Comparison of T1-weighted in- and out-of-phase single shot magnetization-prepared gradient-recalled-echo with three-dimensional gradient-recalled-echo at 3.0 Tesla: preliminary observations in abdominal studies. *J Magn Reson Imaging* 2012; **35**: 1187-1195 [PMID: 22128047 DOI: 10.1002/jmri.23518]
35 **Herédia V**, Ramalho M, de Campos RO, Lee CH, Dale B, Vaidean GD, Semelka RC. Comparison of a single shot T1-weighted in- and out-of-phase magnetization prepared gradient recalled echo with a standard two-dimensional gradient recalled echo: preliminary findings. *J Magn Reson Imaging* 2011; **33**: 1482-1490 [PMID: 21591019 DOI: 10.1002/jmri.22572]
36 **Semelka RC**, Sofka CM. Hepatic hemangiomas. *Magn Reson Imaging Clin N Am* 1997; **5**: 241-253 [PMID: 9113674]
37 **Lewis S**, Aljarallah B, Trivedi A, Thung SN. Magnetic resonance imaging of a small vessel hepatic hemangioma in a cirrhotic patient with histopathologic correlation. *Clin Imaging* 2015; **39**: 702-706 [PMID: 25748474 DOI: 10.1016/j.clinimag.2015.02.007]
38 **Caseiro-Alves F**, Brito J, Araujo AE, Belo-Soares P, Rodrigues H, Cipriano A, Sousa D, Mathieu D. Liver haemangioma: common and uncommon findings and how to improve the differential diagnosis. *Eur Radiol* 2007; **17**: 1544-1554 [PMID: 17260159 DOI: 10.1007/s00330-006-0503-z]
39 **Semelka RC**, Brown ED, Ascher SM, Patt RH, Bagley AS, Li W, Edelman RR, Shoenut JP, Brown JJ. Hepatic hemangiomas: a multi-institutional study of appearance on T2-weighted and serial gadolinium-enhanced gradient-echo MR images. *Radiology* 1994; **192**: 401-406 [PMID: 8029404 DOI: 10.1148/radiology.192.2.8029404]
40 **Sousa MS**, Ramalho M, Herédia V, Matos AP, Palas J, Jeon YH, Afonso D, Semelka RC. Perilesional enhancement of liver cavernous hemangiomas in magnetic resonance imaging. *Abdom Imaging* 2014; **39**: 722-730 [PMID: 24531350 DOI: 10.1007/s00261-014-0100-6]
41 **Klotz T**, Montoriol PF, Da Ines D, Petitcolin V, Joubert-Zakeyh J, Garcier JM. Hepatic haemangioma: common and uncommon imaging features. *Diagn Interv Imaging* 2013; **94**: 849-859 [PMID: 23796395 DOI: 10.1016/j.diii.2013.04.008]
42 **Nahm CB**, Ng K, Lockie P, Samra JS, Hugh TJ. Focal nodular hyperplasia--a review of myths and truths. *J Gastrointest Surg* 2011; **15**: 2275-2283 [PMID: 21959783 DOI: 10.1007/s11605-011-1680-x]
43 **Marin D**, Brancatelli G, Federle MP, Lagalla R, Catalano C, Passariello R, Midiri M, Vilgrain V. Focal nodular hyperplasia: typical and atypical MRI findings with emphasis on the use of contrast media. *Clin Radiol* 2008; **63**: 577-585 [PMID: 18374723 DOI: 10.1016/j.crad.2007.06.011]
44 **Ronot M**, Vilgrain V. Imaging of benign hepatocellular lesions: current concepts and recent updates. *Clin Res Hepatol Gastroenterol* 2014; **38**: 681-688 [PMID: 24636468 DOI: 10.1016/j.clinre.2014.01.014]
45 **van Kessel CS**, de Boer E, ten Kate FJ, Brosens LA, Veldhuis WB, van Leeuwen MS. Focal nodular hyperplasia: hepatobiliary enhancement patterns on gadoxetic-acid contrast-enhanced MRI. *Abdom Imaging* 2013; **38**: 490-501 [PMID: 22729462 DOI:

10.1007/s00261-012-9916-0]
46 **Zucman-Rossi J**, Jeannot E, Nhieu JT, Scoazec JY, Guettier C, Rebouissou S, Bacq Y, Leteurtre E, Paradis V, Michalak S, Wendum D, Chiche L, Fabre M, Mellottee L, Laurent C, Partensky C, Castaing D, Zafrani ES, Laurent-Puig P, Balabaud C, Bioulac-Sage P. Genotype-phenotype correlation in hepatocellular adenoma: new classification and relationship with HCC. *Hepatology* 2006; **43**: 515-524 [PMID: 16496320 DOI: 10.1002/hep.21068]
47 **van Aalten SM**, Thomeer MG, Terkivatan T, Dwarkasing RS, Verheij J, de Man RA, Ijzermans JN. Hepatocellular adenomas: correlation of MR imaging findings with pathologic subtype classification. *Radiology* 2011; **261**: 172-181 [PMID: 21875850 DOI: 10.1148/radiol.11110023]
48 **Stoot JH**, Coelen RJ, De Jong MC, Dejong CH. Malignant transformation of hepatocellular adenomas into hepatocellular carcinomas: a systematic review including more than 1600 adenoma cases. *HPB* (Oxford) 2010; **12**: 509-522 [PMID: 20887318 DOI: 10.1111/j.1477-2574.2010.00222.x]
49 **Laumonier H**, Cailliez H, Balabaud C, Possenti L, Zucman-Rossi J, Bioulac-Sage P, Trillaud H. Role of contrast-enhanced sonography in differentiation of subtypes of hepatocellular adenoma: correlation with MRI findings. *AJR Am J Roentgenol* 2012; **199**: 341-348 [PMID: 22826395 DOI: 10.2214/AJR.11.7046]
50 **Kim MJ**, Rhee HJ, Jeong HT. Hyperintense lesions on gadoxetate disodium-enhanced hepatobiliary phase imaging. *AJR Am J Roentgenol* 2012; **199**: W575-W586 [PMID: 23096201 DOI: 10.2214/AJR.11.8205]
51 **Vachha B**, Sun MR, Siewert B, Eisenberg RL. Cystic lesions of the liver. *AJR Am J Roentgenol* 2011; **196**: W355-W366 [PMID: 21427297 DOI: 10.2214/AJR.10.5292]
52 **Borhani AA**, Wiant A, Heller MT. Cystic hepatic lesions: a review and an algorithmic approach. *AJR Am J Roentgenol* 2014; **203**: 1192-1204 [PMID: 25415696 DOI: 10.2214/AJR.13.12386]
53 **Semelka RC**, Hussain SM, Marcos HB, Woosley JT. Biliary hamartomas: solitary and multiple lesions shown on current MR techniques including gadolinium enhancement. *J Magn Reson Imaging* 1999; **10**: 196-201 [PMID: 10441025 DOI: 10.1002/(SICI)1522-2586(199908)10:2<196::AID-JMRI14>3.0.CO;2-R]
54 **Mezhir JJ**, Fong Y, Jacks LM, Getrajdman GI, Brody LA, Covey AM, Thornton RH, Jarnagin WR, Solomon SB, Brown KT. Current management of pyogenic liver abscess: surgery is now second-line treatment. *J Am Coll Surg* 2010; **210**: 975-983 [PMID: 20510807 DOI: 10.1016/j.jamcollsurg.2010.03.004]
55 **Qian LJ**, Zhu J, Zhuang ZG, Xia Q, Liu Q, Xu JR. Spectrum of multilocular cystic hepatic lesions: CT and MR imaging findings with pathologic correlation. *Radiographics* 2013; **33**: 1419-1433 [PMID: 24025933 DOI: 10.1148/rg.335125063]
56 **El-Serag HB**, Rudolph KL. Hepatocellular carcinoma: epidemiology and molecular carcinogenesis. *Gastroenterology* 2007; **132**: 2557-2576 [PMID: 17570226 DOI: 10.1053/j.gastro.2007.04.061]
57 **van den Bos IC**, Hussain SM, de Man RA, Zondervan PE, Ijzermans JN, Krestin GP. Primary hepatocellular lesions: imaging findings on state-of-the-art magnetic resonance imaging, with pathologic correlation. *Curr Probl Diagn Radiol* 2008; **37**: 104-114 [PMID: 18436110 DOI: 10.1067/j.cpradiol.2007.07.003]
58 **Kudo M**. Multistep human hepatocarcinogenesis: correlation of imaging with pathology. *J Gastroenterol* 2009; **44 Suppl 19**: 112-118 [PMID: 19148804 DOI: 10.1007/s00535-008-2274-6]
59 **Ayuso C**, Rimola J, García-Criado A. Imaging of HCC. *Abdom Imaging* 2012; **37**: 215-230 [PMID: 21909721 DOI: 10.1007/s00261-011-9794-x]
60 **Becker-Weidman DJ**, Kalb B, Sharma P, Kitajima HD, Lurie CR, Chen Z, Spivey JR, Knechtle SJ, Hanish SI, Adsay NV, Farris AB, Martin DR. Hepatocellular carcinoma lesion characterization: single-institution clinical performance review of multiphase gadolinium-enhanced MR imaging--comparison to prior same-center results after MR systems improvements. *Radiology* 2011; **261**: 824-833 [PMID: 21969663 DOI: 10.1148/radiol.11110157]
61 **El-Serag HB**, Marrero JA, Rudolph L, Reddy KR. Diagnosis and treatment of hepatocellular carcinoma. *Gastroenterology* 2008; **134**: 1752-1763 [PMID: 18471552 DOI: 10.1053/j.gastro.2008.02.090]
62 **Hussain SM**, Semelka RC. Liver masses. *Magn Reson Imaging Clin N Am* 2005; **13**: 255-275 [PMID: 15935311 DOI: 10.1016/j.mric.2005.03.007]
63 **Bruix J**, Sherman M. Management of hepatocellular carcinoma: an update. *Hepatology* 2011; **53**: 1020-1022 [PMID: 21374666 DOI: 10.1002/hep.24199]
64 **Kwon HJ**, Byun JH, Kim JY, Hong GS, Won HJ, Shin YM, Kim PN. Differentiation of small (≤2 cm) hepatocellular carcinomas from small benign nodules in cirrhotic liver on gadoxetic acid-enhanced and diffusion-weighted magnetic resonance images. *Abdom Imaging* 2015; **40**: 64-75 [PMID: 24997560 DOI: 10.1007/s00261-014-0188-8]
65 **Hwang J**, Kim SH, Lee MW, Lee JY. Small (≤ 2 cm) hepatocellular carcinoma in patients with chronic liver disease: comparison of gadoxetic acid-enhanced 3.0 T MRI and multiphasic 64-multirow detector CT. *Br J Radiol* 2012; **85**: e314-e322 [PMID: 22167508 DOI: 10.1259/bjr/27727228]
66 **Kim MJ**, Lee M, Choi JY, Park YN. Imaging features of small hepatocellular carcinomas with microvascular invasion on gadoxetic acid-enhanced MR imaging. *Eur J Radiol* 2012; **81**: 2507-2512 [PMID: 22137613 DOI: 10.1016/j.ejrad.2011.11.014]
67 **Hwang J**, Kim YK, Jeong WK, Choi D, Rhim H, Lee WJ. Nonhypervascular Hypointense Nodules at Gadoxetic Acid-enhanced MR Imaging in Chronic Liver Disease: Diffusion-weighted Imaging for Characterization. *Radiology* 2015; **276**: 137-146 [PMID: 25734551 DOI: 10.1148/radiol.15141350]
68 **Sirlin CB**, Hussain HK, Jonas E, Kanematsu M, Min Lee J, Merkle EM, Peck-Radosavljevic M, Reeder SB, Ricke J, Sakamoto M. Consensus report from the 6th International forum for liver MRI using gadoxetic acid. *J Magn Reson Imaging* 2014; **40**: 516-529 [PMID: 24923695 DOI: 10.1002/jmri.24419]
69 **Ahn SS**, Kim MJ, Lim JS, Hong HS, Chung YE, Choi JY. Added value of gadoxetic acid-enhanced hepatobiliary phase MR imaging in the diagnosis of hepatocellular carcinoma. *Radiology* 2010; **255**: 459-466 [PMID: 20413759 DOI: 10.1148/radiol.10091388]
70 **Kim TK**, Lee KH, Jang HJ, Haider MA, Jacks LM, Menezes RJ, Park SH, Yazdi L, Sherman M, Khalili K. Analysis of gadobenate dimeglumine-enhanced MR findings for characterizing small (1-2-cm) hepatic nodules in patients at high risk for hepatocellular carcinoma. *Radiology* 2011; **259**: 730-738 [PMID: 21364083 DOI: 10.1148/radiol.11101549]
71 **Sano K**, Ichikawa T, Motosugi U, Sou H, Muhi AM, Matsuda M, Nakano M, Sakamoto M, Nakazawa T, Asakawa M, Fujii H, Kitamura T, Enomoto N, Araki T. Imaging study of early hepatocellular carcinoma: usefulness of gadoxetic acid-enhanced MR imaging. *Radiology* 2011; **261**: 834-844 [PMID: 21998047 DOI: 10.1148/radiol.11101840]
72 **Park MJ**, Kim YK, Lee MW, Lee WJ, Kim YS, Kim SH, Choi D, Rhim H. Small hepatocellular carcinomas: improved sensitivity by combining gadoxetic acid-enhanced and diffusion-weighted MR imaging patterns. *Radiology* 2012; **264**: 761-770 [PMID: 22843769 DOI: 10.1148/radiol.12112517]
73 **Akai H**, Kiryu S, Matsuda I, Satou J, Takao H, Tajima T, Watanabe Y, Imamura H, Kokudo N, Akahane M, Ohtomo K. Detection of hepatocellular carcinoma by Gd-EOB-DTPA-enhanced liver MRI: comparison with triple phase 64 detector row helical CT. *Eur J Radiol* 2011; **80**: 310-315 [PMID: 20732773 DOI: 10.1016/j.ejrad.2010.07.026]
74 **Baek CK**, Choi JY, Kim KA, Park MS, Lim JS, Chung YE, Kim MJ, Kim KW. Hepatocellular carcinoma in patients with chronic liver disease: a comparison of gadoxetic acid-enhanced MRI and multiphasic MDCT. *Clin Radiol* 2012; **67**: 148-156 [PMID: 21920517 DOI: 10.1016/j.crad.2011.08.011]
75 **Kim SH**, Kim SH, Lee J, Kim MJ, Jeon YH, Park Y, Choi D, Lee WJ, Lim HK. Gadoxetic acid-enhanced MRI versus triple-phase MDCT for the preoperative detection of hepatocellular carcinoma. *AJR Am J Roentgenol* 2009; **192**: 1675-1681 [PMID: 19457834 DOI: 10.2214/AJR.08.1262]
76 **Onishi H**, Kim T, Imai Y, Hori M, Nagano H, Nakaya Y, Tsuboyama T, Nakamoto A, Tatsumi M, Kumano S, Okada M, Takamura M, Wakasa K, Tomiyama N, Murakami T. Hypervascular hepatocellular carcinomas: detection with gadoxetate disodium-enhanced MR imaging and multiphasic multidetector CT. *Eur*

Radiol 2012; **22**: 845-854 [PMID: 22057248 DOI: 10.1007/s00330-011-2316-y]
77 **Sun HY**, Lee JM, Shin CI, Lee DH, Moon SK, Kim KW, Han JK, Choi BI. Gadoxetic acid-enhanced magnetic resonance imaging for differentiating small hepatocellular carcinomas (< or =2 cm in diameter) from arterial enhancing pseudolesions: special emphasis on hepatobiliary phase imaging. *Invest Radiol* 2010; **45**: 96-103 [PMID: 20057319 DOI: 10.1097/RLI.0b013e3181c5faf7]
78 **Liu X**, Zou L, Liu F, Zhou Y, Song B. Gadoxetic acid disodium-enhanced magnetic resonance imaging for the detection of hepatocellular carcinoma: a meta-analysis. *PLoS One* 2013; **8**: e70896 [PMID: 23967130 DOI: 10.1371/journal.pone.0070896]
79 **Wu LM**, Xu JR, Gu HY, Hua J, Chen J, Zhu J, Zhang W, Hu J. Is liver-specific gadoxetic acid-enhanced magnetic resonance imaging a reliable tool for detection of hepatocellular carcinoma in patients with chronic liver disease? *Dig Dis Sci* 2013; **58**: 3313-3325 [PMID: 23884757 DOI: 10.1007/s10620-013-2790-y]
80 **Jha RC**, Zanello PA, Nguyen XM, Pehlivanova M, Johnson LB, Fishbein T, Shetty K. Small hepatocellular carcinoma: MRI findings for predicting tumor growth rates. *Acad Radiol* 2014; **21**: 1455-1464 [PMID: 25300723 DOI: 10.1016/j.acra.2014.06.011]
81 **Parente DB**, Perez RM, Eiras-Araujo A, Oliveira Neto JA, Marchiori E, Constantino CP, Amorim VB, Rodrigues RS. MR imaging of hypervascular lesions in the cirrhotic liver: a diagnostic dilemma. *Radiographics* 2012; **32**: 767-787 [PMID: 22582358 DOI: 10.1148/rg.323115131]
82 **Roth CG**, Mitchell DG. Hepatocellular carcinoma and other hepatic malignancies: MR imaging. *Radiol Clin North Am* 2014; **52**: 683-707 [PMID: 24889167 DOI: 10.1016/j.rcl.2014.02.015]
83 **Jhaveri KS**, Hosseini-Nik H. MRI of cholangiocarcinoma. *J Magn Reson Imaging* 2014; Epub ahead of print [PMID: 25447417 DOI: 10.1002/jmri.24810]
84 **Al Ansari N**, Kim BS, Srirattanapong S, Semelka CT, Ramalho M, Altun E, Woosley JT, Calvo B, Semelka RC. Mass-forming cholangiocarcinoma and adenocarcinoma of unknown primary: can they be distinguished on liver MRI? *Abdom Imaging* 2014; **39**: 1228-1240 [PMID: 24929668 DOI: 10.1007/s00261-014-0172-3]
85 **Park HS**, Lee JM, Choi JY, Lee MW, Kim HJ, Han JK, Choi BI. Preoperative evaluation of bile duct cancer: MRI combined with MR cholangiopancreatography versus MDCT with direct cholangiography. *AJR Am J Roentgenol* 2008; **190**: 396-405 [PMID: 18212225 DOI: 10.2214/AJR.07.2310]
86 **Nanashima A**, Sumida Y, Abo T, Oikawa M, Murakami G, Takeshita H, Fukuoka H, Hidaka S, Nagayasu T, Sakamoto I, Sawai T. Relationship between pattern of tumor enhancement and clinicopathologic characteristics in intrahepatic cholangiocarcinoma. *J Surg Oncol* 2008; **98**: 535-539 [PMID: 18814285 DOI: 10.1002/jso.21142]
87 **Kim SA**, Lee JM, Lee KB, Kim SH, Yoon SH, Han JK, Choi BI. Intrahepatic mass-forming cholangiocarcinomas: enhancement patterns at multiphasic CT, with special emphasis on arterial enhancement pattern--correlation with clinicopathologic findings. *Radiology* 2011; **260**: 148-157 [PMID: 21474703 DOI: 10.1148/radiol.11101777/-/DC1]
88 **Ariizumi S**, Kotera Y, Takahashi Y, Katagiri S, Chen IP, Ota T, Yamamoto M. Mass-forming intrahepatic cholangiocarcinoma with marked enhancement on arterial-phase computed tomography reflects favorable surgical outcomes. *J Surg Oncol* 2011; **104**: 130-139 [PMID: 21448898 DOI: 10.1002/jso.21917]
89 **Vilana R**, Forner A, Bianchi L, García-Criado A, Rimola J, de Lope CR, Reig M, Ayuso C, Brú C, Bruix J. Intrahepatic peripheral cholangiocarcinoma in cirrhosis patients may display a vascular pattern similar to hepatocellular carcinoma on contrast-enhanced ultrasound. *Hepatology* 2010; **51**: 2020-2029 [PMID: 20512990 DOI: 10.1002/hep.23600]
90 **Xu J**, Igarashi S, Sasaki M, Matsubara T, Yoneda N, Kozaka K, Ikeda H, Kim J, Yu E, Matsui O, Nakanuma Y. Intrahepatic cholangiocarcinomas in cirrhosis are hypervascular in comparison with those in normal livers. *Liver Int* 2012; **32**: 1156-1164 [PMID: 22417172 DOI: 10.1111/j.1478-3231.2012.02783.x]
91 **Jeong HT**, Kim MJ, Chung YE, Choi JY, Park YN, Kim KW. Gadoxetate disodium-enhanced MRI of mass-forming intrahepatic cholangiocarcinomas: imaging-histologic correlation. *AJR Am J Roentgenol* 2013; **201**: W603-W611 [PMID: 24059399 DOI: 10.2214/AJR.12.10262]
92 **Kang Y**, Lee JM, Kim SH, Han JK, Choi BI. Intrahepatic mass-forming cholangiocarcinoma: enhancement patterns on gadoxetic acid-enhanced MR images. *Radiology* 2012; **264**: 751-760 [PMID: 22798225 DOI: 10.1148/radiol.12112308]
93 **Péporté AR**, Sommer WH, Nikolaou K, Reiser MF, Zech CJ. Imaging features of intrahepatic cholangiocarcinoma in Gd-EOB-DTPA-enhanced MRI. *Eur J Radiol* 2013; **82**: e101-e106 [PMID: 23159401 DOI: 10.1016/j.ejrad.2012.10.010]
94 **Koh DM**, Brown G, Riddell AM, Scurr E, Collins DJ, Allen SD, Chau I, Cunningham D, deSouza NM, Leach MO, Husband JE. Detection of colorectal hepatic metastases using MnDPDP MR imaging and diffusion-weighted imaging (DWI) alone and in combination. *Eur Radiol* 2008; **18**: 903-910 [PMID: 18193234 DOI: 10.1007/s00330-007-0847-z]
95 **Donati OF**, Fischer MA, Chuck N, Hunziker R, Weishaupt D, Reiner CS. Accuracy and confidence of Gd-EOB-DTPA enhanced MRI and diffusion-weighted imaging alone and in combination for the diagnosis of liver metastases. *Eur J Radiol* 2013; **82**: 822-828 [PMID: 23287713 DOI: 10.1016/j.ejrad.2012.12.005]
96 **Böttcher J**, Hansch A, Pfeil A, Schmidt P, Malich A, Schneeweiss A, Maurer MH, Streitparth F, Teichgräber UK, Renz DM. Detection and classification of different liver lesions: comparison of Gd-EOB-DTPA-enhanced MRI versus multiphasic spiral CT in a clinical single centre investigation. *Eur J Radiol* 2013; **82**: 1860-1869 [PMID: 23932636 DOI: 10.1016/j.ejrad.2013.06.013]
97 **Kim YK**, Lee MW, Lee WJ, Kim SH, Rhim H, Lim JH, Choi D, Kim YS, Jang KM, Lee SJ, Lim HK. Diagnostic accuracy and sensitivity of diffusion-weighted and of gadoxetic acid-enhanced 3-T MR imaging alone or in combination in the detection of small liver metastasis (≤ 1.5 cm in diameter). *Invest Radiol* 2012; **47**: 159-166 [PMID: 22330426 DOI: 10.1097/RLI.0b013e31823a1495]
98 **De Bruyne S**, Van Damme N, Smeets P, Ferdinande L, Ceelen W, Mertens J, Van de Wiele C, Troisi R, Libbrecht L, Laurent S, Geboes K, Peeters M. Value of DCE-MRI and FDG-PET/CT in the prediction of response to preoperative chemotherapy with bevacizumab for colorectal liver metastases. *Br J Cancer* 2012; **106**: 1926-1933 [PMID: 22596235 DOI: 10.1038/bjc.2012.184]
99 **Kulemann V**, Schima W, Tamandl D, Kaczirek K, Gruenberger T, Wrba F, Weber M, Ba-Ssalamah A. Preoperative detection of colorectal liver metastases in fatty liver: MDCT or MRI? *Eur J Radiol* 2011; **79**: e1-e6 [PMID: 20392584 DOI: 10.1016/j.ejrad.2010.03.004]
100 **O'Connor JP**, Rose CJ, Jackson A, Watson Y, Cheung S, Maders F, Whitcher BJ, Roberts C, Buonaccorsi GA, Thompson G, Clamp AR, Jayson GC, Parker GJ. DCE-MRI biomarkers of tumour heterogeneity predict CRC liver metastasis shrinkage following bevacizumab and FOLFOX-6. *Br J Cancer* 2011; **105**: 139-145 [PMID: 21673686 DOI: 10.1038/bjc.2011.191]
101 **Lewin M**, Handra-Luca A, Arrivé L, Wendum D, Paradis V, Bridel E, Fléjou JF, Belghiti J, Tubiana JM, Vilgrain V. Liver adenomatosis: classification of MR imaging features and comparison with pathologic findings. *Radiology* 2006; **241**: 433-440 [PMID: 16966481 DOI: 10.1148/radiol.2412051243]

P- Reviewer: Fouad YM, He ST, José MG, Sergi C, Sonzogni A
S- Editor: Tian YL **L- Editor**: A **E- Editor**: Liu SQ

Published by **Baishideng Publishing Group Inc**
8226 Regency Drive, Pleasanton, CA 94588, USA
Telephone: +1-925-223-8242
Fax: +1-925-223-8243
E-mail: bpgoffice@wjgnet.com
Help Desk: http://www.wjgnet.com/esps/helpdesk.aspx
http://www.wjgnet.com